Journal of
Composites Science

MDPI

Review

Progressive Review of Functional Nanomaterials-Based Polymer Nanocomposites for Efficient EMI Shielding

Prashanth Kallambadi Sadashivappa [1], Revathi Venkatachalam [1], Ramyakrishna Pothu [2], Rajender Boddula [3,*], Prasun Banerjee [4], Ramachandra Naik [1,*], Ahmed Bahgat Radwan [3] and Noora Al-Qahtani [3,*]

1 Department of Physics, New Horizon College of Engineering, Bangalore 560103, India
2 School of Physics and Electronics, College of Chemistry and Chemical Engineering, Hunan University, Changsha 410082, China
3 Center for Advanced Materials (CAM), Qatar University, Doha P.O. Box 2713, Qatar
4 Multiferroic and Magnetic Material Research Laboratory, Gandhi Institute of Technology and Management (GITAM) University, Bengaluru 561203, India
* Correspondence: research.raaj@gmail.com (R.B.); rcnaikphysics@gmail.com (R.N.); noora.alqahtani@qu.edu.qa (N.A.-Q.)

Abstract: Nanomaterials have assumed an imperative part in the advancement of human evolution and are more intertwined in our thinking and application. Contrary to the conventional micron-filled composites, the unique nanofillers often modify the properties of the polymer matrix at the same time, bestowing new functionality because of their chemical composition and their nano dimensions. The unprecedented technological revolution is driving people to adapt to miniaturized electronic gadgets. The sources of electromagnetic fields are ubiquitous in a tech-driven society. The COVID-19 pandemic has escalated the proliferation of electromagnetic interference as the world embraced remote working and content delivery over mobile communication devices. While EMI shielding is performed using the combination of reflection, absorption, and electrical and magnetic properties, under certain considerations, the dominant nature of any one of the properties may be required. The miniaturization of electronic gadgets coupled with wireless technologies is driving us to search for alternate lightweight EMI shielding materials with improved functionalities relative to conventional metals. Polymer nanocomposites have emerged as functional materials with versatile properties for EMI shielding. This paper reviews nanomaterials-based polymer nanocomposites for EMI shielding applications.

Keywords: EMI shielding; polymer nanocomposites; metamaterials; carbon nanotubes; 2D nanomaterials

Citation: Kallambadi Sadashivappa, P.; Venkatachalam, R.; Pothu, R.; Boddula, R.; Banerjee, P.; Naik, R.; Radwan, A.B.; Al-Qahtani, N. Progressive Review of Functional Nanomaterials-Based Polymer Nanocomposites for Efficient EMI Shielding. *J. Compos. Sci.* **2023**, *7*, 77. https://doi.org/10.3390/jcs7020077

Academic Editor: Francesco Tornabene

Received: 30 December 2022
Revised: 2 February 2023
Accepted: 10 February 2023
Published: 13 February 2023

1. Introduction

Technology changes and upgradation are making electronic devices redundant in a few months and driving the miniaturization of electronic gadgets unprecedentedly. The sources of electromagnetic fields are ubiquitous in a tech-driven society. The COVID-19 pandemic has escalated the proliferation of electromagnetic interference as the world embraced remote working and content delivery over mobile communication devices. Electromagnetic interference (EMI) shielding [1] is an important area on which there is continuous focus either to improve the bandwidth or geometric and physical properties of the shielding. With novel requirements such as flexibility, being lightweight, and tunability, new materials are being developed based on polymer composites. The choice of fillers plays a very significant role in shielding. While EMI shielding is performed using the combination of reflection, absorption, electrical and magnetic properties, under certain considerations, the dominant nature of any one of the properties may be required. For example, in the case of unwanted sources existing within the housing of the electronic circuit, a thin absorber is needed, while it may be fine to have a reflection-based one if the source is outside. Once again, depending on the hazardous nature of the external source, absorbers play a significant role. Therefore,

more emphasis is put on the absorption nature of EMI shielding. The development of communication devices has pushed the operating frequency range to higher frequencies than the conventional 900 MHz and 2.4 GHz operations. Aiming for frequencies higher than 5 GHz for higher bandwidth and speed of operation has resulted in the requirement of broadband EMI shielding structures [1–3].

The present situation warrants the use of multiple bands embedded within a communication device suitable for Wifi, Bluetooth, mobile communication, etc. The interference to these devices from external sources and internal sources is not negligible. Therefore, one has to develop shielding structures that can be used for all these frequency regions or simply look for broadband-shielding structures. Historically, metal-based composites were used as the predominant material for EMI shielding by the virtue of their superior electrical conductivity, mechanical properties, and permeability [4], however, they were met with challenges of corrosion and lack of mechanical flexibility by the metallic fillers. To meet the criterion of paramount EMI shielding effectiveness, tailored functional materials with outstanding properties are designed for efficient EMI shielding. Reflection, which is the primary mechanism of shielding, must have enough electrical conductivity, and the secondary mechanism due to absorption comes from the inherent interaction of the radiation arising out of the electric and magnetic dipoles [5] with the incident radiation. The penetration depth of the radiation assumes significance in this aspect. With a higher level of absorption resulting in the thickness of the material being greater than the penetration depth, the absorption increases exponentially with an increase in thickness. When the penetration depth is higher than the thickness of the sample, the multiple reflections between the front and back interfaces increase the path length, thereby enhancing the total absorption. For every reflection into the bulk of the material at the interfaces, the amount of absorption enhances the shielding exponentially.

Reflection-dominant shielding materials give rise to the secondary interference of EM waves with the mere deflection of EM waves; alternately the absorption dominant shielding materials eliminates EM waves through ohmic and thermal losses [5–7]. To reach this goal of creating materials with the required attributes, a wide range of polymer nanocomposites are desired for EMI shielding with adequate impedance matching, high attenuation capabilities, wider absorbing bandwidth, lower thickness, and good thermal conductivity [8–11]. In the case of nano-composites, the presence of scatterers as fillers improves the path length. This would enhance the shielding due to absorption. The shielding effectiveness due to reflection is a function of the ratio of conductivity and permeability of the material. The shielding effectiveness due to absorption depends upon the thickness and attenuation constant of the material. Additionally, reflections at numerous interfaces inside the material also contribute to the shielding effectiveness, which depends on the sample thickness. The multiple reflections depend on the sample thickness. [12]. The excellent EMI shielding material possesses outstanding impedance-matching attributes which depend on the permittivity and permeability. The size, thickness, and shape of the nanomaterials impact the permeability and henceforth result in shielding effectiveness [13–15].

Over the years, a wide range of polymer composites has been explored for EMI shielding. In the last decade, the emergence of nanomaterials with a multitude of functionalities enabled various researchers to explore the possibilities of polymer nanocomposites for EMI shielding. The ease of dispersion of carbonaceous fillers in the macromolecular matrix and the resulting manifestation of the conductive network make the Carbon-based fillers one of the ideal candidates for lightweight EMI shielding materials [16] Several polymer nanocomposites with prudent blends of fillers, such as carbon nanofibers, carbon nanotubes, metal nanowires, graphene, reduced graphene oxide, hBN MoS_2, MXene, and magnetic fillers Fe_3O_4, Fe_2O_3, and nickel ferrite [17] have been extensively used for designing efficient EMI shielding materials. The published review articles pertain to standalone polymer-carbon nanotubes, polymer–graphene materials, and admixtures of various 2D nanomaterials. Our review focuses on various polymers blended with carbon nanotubes of various weight fractions, with graphene

as the reinforcement material in the macromolecular matrix, and more significantly emerging 2D nanomaterials-based polymer nanocomposites.

2. EMI Shielding Measurements

As a result of exhaustive technological growth, we encounter electromagnetic interference, a kind of pollution due to which the performance of the system is affected [1]. If this problem is not tackled appropriately, it may affect the system and cause the malfunction of devices. It also has an adverse effect on the health of human beings, such as languidness, insomnia, nervousness, and headaches [2]. For the past two decades, sincere efforts are being carried out to reduce electromagnetic interference (EMI) by adopting various techniques and materials such as metals, polymers, and dielectric and magnetic materials.

When an EM wave passes through a barrier, it can be absorbed and reflected by the barrier. The remaining energy which is neither absorbed nor reflected is termed the residual energy, which comes out of the shield. The effectiveness of a shield, which is a measurable quantity, is given in terms of shielding effectiveness that can be given by the following equations [3]:

$$SE_T = SE_R + SE_A + SE_M = 10 \log_{10} (P_T/P_I) \quad (1a)$$

$$SE_T = 20 \log_{10} (E_T/E_I) = 20 \log_{10} (H_T/H_I) \quad (1b)$$

In the above Equation (1a), P_I and P_T are the power of incident and transmitted EM waves, respectively. E_I, E_T is the corresponding electric field intensity and H_I, H_T is the corresponding magnetic field intensity. The term SE_R is shielding effectiveness due to reflection, SE_A is shielding effectiveness due to absorption, and SE_M is shielding effectiveness due to multiple reflections. The graphical representation of EMI shielding is represented by (Figure 1) [4]. Using scattering parameters, also known as S-parameters S_{11} (or S_{22}) and S_{12} (or S_{21}) the incident and the transmitted waves, respectively, can be represented in a two port vector network analyzer. This can, in turn, be related to reflectance (R) and transmittance (T):

$$T = |E_T/E_I|^2 = |S_{12}|^2 = |S_{21}|^2 \quad (1c)$$

$$R = |E_R/E_I|^2 = |S_{11}|^2 = |S_{22}|^2 \quad (1d)$$

The absorbance is therefore given by

$$A = (1 - R - T) \quad (1e)$$

The losses due to reflection and absorption can be represented as,

$$SE_R = 10\log (1 - R) \quad (1f)$$

$$SE_A = 10\log (1 - A_{eff}) = 10\log [T/(1 - R)] \quad (1g)$$

Therefore, a vector network analyzer can calculate the loss components due to transmission and reflection. A prudent examination of the shielding expressions shows that a proper shield should have either mobile charge carriers or dipoles which can interact with electric and magnetic vectors of the incident radiation [12]. Therefore, metals are preferred as shielding materials due to their good conductivity [18], but they also have their demerits, such as high reflectivity, that they are easily prone to corrosion, heaviness, and high processing cost [4].

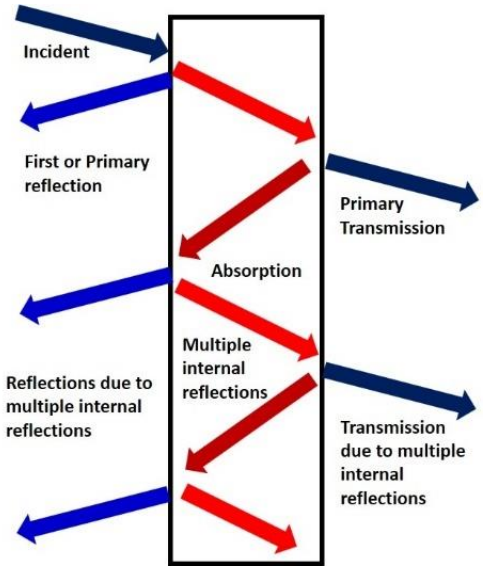

Figure 1. Graphical representation of EMI shielding [19,20].

3. EMI Shielding Materials

EMI shielding encompasses the blockage of EMF, using shields made of conductive or magnetic materials [3]. The word shield usually refers to an enclosure that functions as a barricade against electromagnetic radiation. Shielding effectiveness, which is a function of frequency [1], can be measured quantitatively by obtaining the ratio of the impinging energy to the remanent energy.

A single material by itself cannot take care of every single aspect of shielding. Various efforts were made by combining suitable materials in proper combination such as composites, alloys, and ceramics, etc. [19,20]. The development of nanomaterials, especially nanocomposites [20], and their wonderful properties also aid in obtaining the best-suited material for EMI shielding (Figure 2). The electrical conductivity and presence of dipoles are quintessential to shielding [19,20]. To reach this goal of creating materials with the required attributes, a wide band of materials is used to obtain nanocomposites [19]. Although polymer nanocomposites are preferred over metals, the process of obtaining the desired electrical and magnetic properties is a challenging one [3].

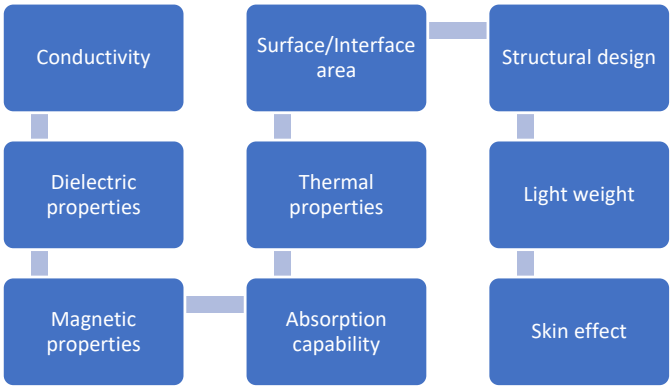

Figure 2. The important attributes of an effective shielding material [21].

Historically, metals were the materials preferred for EMI shielding; nevertheless, metallic materials are susceptible to corrosion, and are heavy, expensive, and prone to wear and tear.

The metallic oxides are excellent shielding materials with apt dielectric constants and magnetic permeability. The availability of dipoles (electric and magnetic) at higher frequencies [22] makes them an attractive option for EMI shielding.

Recently, carbon-based materials such as carbon nanotubes, graphene, graphene oxide (GO), and reduced graphene oxide (rGO) are profoundly used for shielding. The exceptional mechanical properties of two-dimensional (2D) nanomaterials (tensile strength ~130 GPa), and unique electrical properties (mobility~10,000 $Cm^2\ V^{-1}\ S^{-1}$) [11] have made them an ideal candidate as fillers in nanocomposite-based EMI shielding. Amidst the recent growing challenges in EMI shielding, Mxenes have become popular nanomaterials for shielding owing to their structural design and surface area [22].

4. Metamaterials

Metamaterials (MM) are a fantastic class of "artificial materials" that have been engineered to exhibit distinctive qualities that set them apart from naturally occurring materials. Metamaterials are made up of an artificial arrangement of structures that are periodic in nature and sub-wavelength in dimension. These structures can be designed and fabricated using dielectric and conducting materials. Metamaterials, in a way, are synthetic, as they do not occur in a natural process. These Metamaterials are unique in their design, and exhibit fantastic electromagnetic properties which are not possible to create in naturally occurring homogenous materials. By building the material at the macroscopic level with the right arrangement or combination of two or more materials, the exotic properties of these materials are produced. Rodger M. Walser gave the word metamaterial its official name in 1999 [23]. He claims that MM are man-made, three-dimensional composite materials that are periodically constructed so that the performance of the resulting structure is far greater than that of typical composites. The unique features of this MM come from the size, shape, geometry, orientation, and arrangement of the component composites rather than the component composites themselves. The resulting structure can be created to block, absorb, reflect, and scatter electromagnetic waves in a way that is not possible with normal materials by adjusting these characteristics. When properly built, these metamaterials can affect electromagnetic waves in a way that bulk materials cannot [24–26].

With the help of Maxwell equations, some theoretical features of metamaterials can be identified [27]. In the time domain, Maxwell equations are represented as,

$$\nabla \times E = -j\omega\mu H;\ \nabla .D = \rho \tag{2a}$$

$$\nabla \times H = j + j\omega\varepsilon E;\ \nabla .B = 0 \tag{2b}$$

The above equation shall be altered for a plane wave as

$$k \times E = \omega\mu H;\ k \times H = -\omega\varepsilon E \tag{2c}$$

When ε and μ are positive, then E, H, and k form a right-handed orthogonal system. When ε and μ are negative, then Equation (2c) is altered to,

$$k \times E = -\omega\mu H;\ k \times H = \omega\varepsilon E \tag{2d}$$

The above equation represents left-handed materials and their opposite direction and left-hand triplet E, H, and k. The way a system reacts to the electromagnetic field depends on the nature and property of the materials in the system. The macroscopic parameters, such as permeability μ and permittivity ε, of the materials mainly decide the response of the system to electromagnetic fields. Based on this we can classify the materials into following categories. They are,

DPS (double positive material/medium)
ENG (epsilon negative material/medium)
DNG (double negative material/medium)
MNG (mu negative material/medium)

A DPS (double positive material) is a material where both permittivity (ε) and permeability (μ) are positive. These materials are commonly available dielectrics that are

abundant in nature. ENG (epsilon negative material) has the permittivity (ε) negative and permeability (μ) positive. These are called electrical metamaterials. Noble metals fall in this category, and they occur in a limited manner in nature. DNG (double negative material) has a permittivity (ε) and permeability (μ) less than zero, which is negative. They do not occur in nature. They belong to a category called negative index metamaterial, which does not occur in nature and is a man-made material. MNG (mu negative material) is a type of material that has a positive permittivity (ε) and negative permeability (μ). They are also called magnetic metamaterials. The graphical representation of the above material classification is given in (Figure 3) [24,28,29].

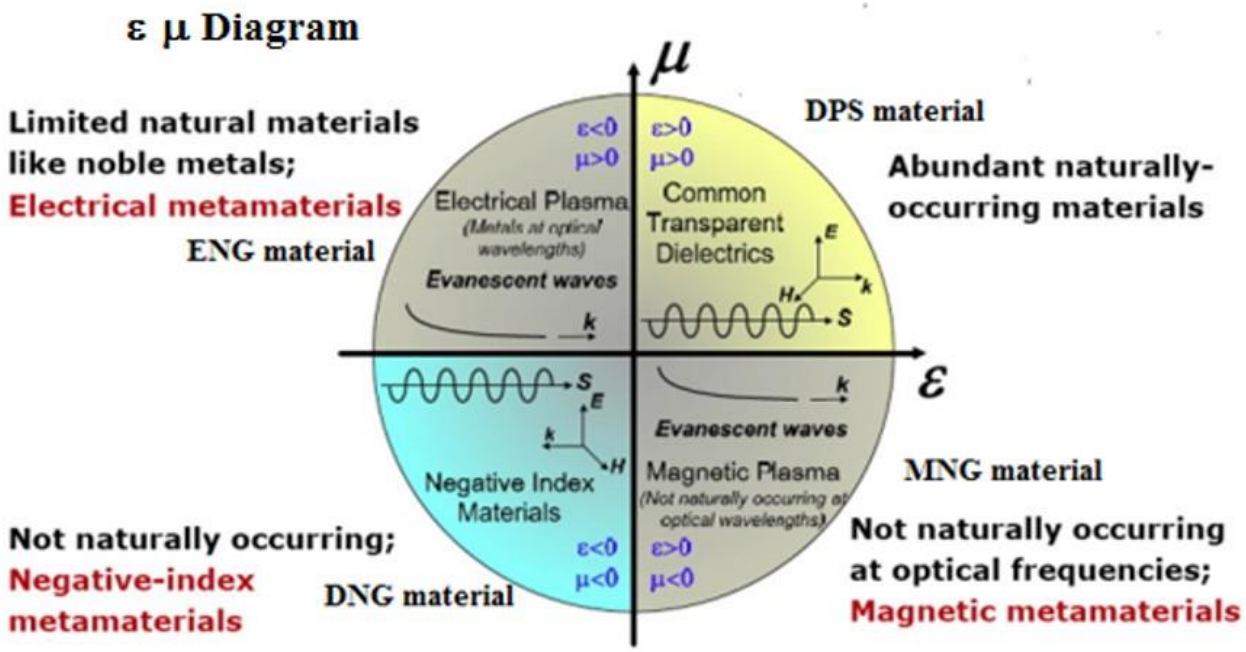

Figure 3. Graphical representation of classification of Metamaterials [29].

Of the above-mentioned metamaterials, the one with both ε and μ negative is called a negative index metamaterial (NIM). The refractive index of these materials is negative. Most of the materials that we come across in optics, such as glass and water, have positive refractive indexes with both permittivity (ε) and permeability (μ) greater than zero. In these materials, the wave propagates in the forward direction. Some man-made engineered materials can have both permittivity and permeability negative, where a backward wave is produced. In some materials either permittivity or permeability is negative but not both. The refractive index of the material is given by

$$n = \mp\sqrt{\varepsilon_r \mu_r} \tag{2e}$$

where

ε_r represents the relative permittivity of the material or medium, and

μ_r represents the relative permeability of the material or medium

In cases where both ε_r, μ_r are negative, the product turns out to be positive and the refractive index is real.

For passive materials to showcase the negative refraction, the real part of ε_r, μ_r need not be negative [29–32].

5. Carbon Nanotubes

Carbon nanotubes (CNT) are a group of nanomaterials that are rolled up graphene sheets with sp2 bonds among carbon molecules. Interestingly, these carbon nanotubes manifest as single-walled (SW) and multi-walled (MW) based on the atomic structural

configuration and side walls. The angle between the bilayers and many layers of graphene has resulted in additional structural forms, namely stacked, herringbone, and bamboo, which comprises an open-ended seamless tube, regular close-ended seamless and stacked seamless cones or cups.

The chemical and structural confirmation, along with the purity and the synthesis route of the carbon nanotubes, defines the properties of the CNTs. They are characterized by a high aspect ratio with diameters less than 100 nm, Young's modulus close to 1 TPa, and tensile strength in the range 11–63 GPa. The chirality and diameter of the CNTs determine the various properties and influences in tailoring the properties of CNTs. They have various applications in electronics, gas sensors, optoelectronics, and nanocomposites. The carbon nanotubes could be metallic or semiconducting with different chemical reactivities owing to their electronic structure. Furthermore, the isotropic, anisotropic, electrical, and mechanical properties in carbon nanotubes depend on the type of bonding in carbon materials. In sp2 hybridized carbon materials, each atom is bonded to only three other atoms in a planar triangular configuration. The excellent attributes of CNTs compared to conventional carbon materials as dispersants in the macromolecular matrix make them suitable for EMI shielding applications, and at a relatively low filling and high shielding, effectiveness could be obtained because of their outstanding mechanical strength, low weight, high aspect ratio, and effortless percolation; thus, it is reasonable to gain a higher conductivity by thinner and longer CNT, because the big networks significantly transfer the electrons within nanocomposite, increasing the conductivity [33] and small diameter. The polymer matrix offers high resistance due to the unavailability of free electrons; however, the electrons in the carbon nanotubes, via tunnelling [34], will be able to overcome the resistance of the macromolecular matrix, forming a three-dimensional conducting network between the filler molecules.

Though CNTs have high electrical conductivity, the prerequisite for the shielding is the attainment of a percolated threshold [34] network with low weight percentage of the CNTs. The Kovacs model [35] suggests tunnelling and interphase regions in polymer nanocomposites with CNTs as fillers have a significant role in offering less interphase resistance, i.e., a thicker and more conductive interphase introduces a more conductive nanocomposite, while a thin and poorly conductive interphase cannot improve the conductivity. As a result, it is important to provide strong interphase regions [34] in PCNT to increase the conductivity. The EMI SE of the polymers/CNTs rely on their hydrophobicity and homogeneous dispersion, method of CNTs' preparation, loading percentage, aspect ratio, and macromolecular matrix. The SE of a few PNCs with CNTs are listed in Table 1.

Table 1. The EMI shielding effectiveness of carbon nanotube-polymer nanocomposites.

Materials	CNT Content	Thickness, t (mm)	EMI SE (dB)	Frequency (GHz)	Ref.
PVDF	4 wt%	0.1	32	10.3	[36]
PU	22 wt%	0.1	20	8–12 (X band)	[37]
PMMA/Epoxy	25 wt%	0.1	20	8–12 (X band)	[38]
PES	6.67 wt%	0.9	30	8–12 (X band)	[39]
TPU/CB-PPy	5–8 wt%	0.5	20	10	[40]
Ppy/CNF/CF	15 wt%	0.65	11.9–52 (multilayered)	S band	[41]

Table 1. *Cont.*

Materials	CNT Content	Thickness, t (mm)	EMI SE (dB)	Frequency (GHz)	Ref.
Epoxy/Nano-Fe_3O_4/ nano FE	5–10 wt%	3	40–100	13–40	[42]
Fe_3O_4/Graphene/CNT	CNT film	0.25	(−44 to −10)	18	[43]
F-CNTS	1:9 wt %	0.0002	(−45)	17.5	[44]
AgFD/TPU/	0.103 vol%	3.4	80	X band	[45]
Silicon rubber/Fe_3O_4	2.08 vol% Fe_3O_4@MWCNTs and 0.81 vol% Ag	-	90	8.2–12.4	[46]
SWNT/GA-chitosan	Up to 40 wt%	10–40	56	X band	[47]
PDMS	1	2.0	46.3	X band	[48]
CNT/PI/PVP	100 *w*/*v* %	3.2	41.1	X band	[49]
PAEK-g-MWCNTs/PEEK	0.372 vol% and 0.496 vol%	-	56	36	[50]
CNT/$BaFe_{12}O_{19}$	2.0 wt%	1.5	(−43.9)	3.9	[51]
CNT/NiNW or CNT/ZnONW in PS	2.0 vol%	1.1	(16.6 to −24.0)	X band	[52]
$CoFe_2O_4$/CNTs	0.34 *w*/*v*%	2	22–25	Ku Band	[53]
SWCNT/$CoFe_2O_4$	10 wt %	2	(−37 to−10)	12.9–7.2	[54]
MWCNTs/ MnZn ferrite/Epoxy	4.0 vol %	2	44	10	[55]
MWCNTs/ $BaFe_{12}O_{19}$	10 wt%	2	(−3.58 to −43.99)	2.56	[56]
CNTs/$BaTiO_3$/PANI	2:3 mass ratio	4	(−30.9 to −10)	7.5 to 10.2	[57]
ABS/MWCNT/CNF/CB	2–15 wt%	1.1	39.9 to 40.7	X band	[58]
PLLA/MWCNT	0.5–10 wt%	2.54	19 to 23	X band	[59]
PANI/MWCNT	5–25 wt%	2	−27.5 to −39.2	Ku band	[60]

6. 2D Nanomaterials

This class of nanomaterials with lateral sizes of more than 100 nm [61] are mostly layered with enhanced specific surface area. As a result of a high specific area, the availability of surface atoms increases manifold, i.e., in comparison with zero-dimensional (0D) and one-dimensional (1D) materials, 2D layered materials possess several extraordinary advantages. 2D layered materials have larger specific surface areas [62] compared to their bulk structures, which in turn provide greater surface energy. The electron confinement in the ultrathin region gives rise to its exceptional electrical properties, covalent bonding for mechanical properties and surface atoms for surface anchoring sites [63–65]. The different types of 2D nanomaterials are listed in (Figure 4). Graphene comprises a monolayer of sp2 hybridized carbon atoms in a hexagonal lattice with a bond length of 0.142 nm. Contrastingly, the other types of 2D nanomaterials, transition metal oxides (TMOs), and transition metal dichalcogenides (TMDs) pose stable single crystal units [66–68] and are listed below in (Figure 5).

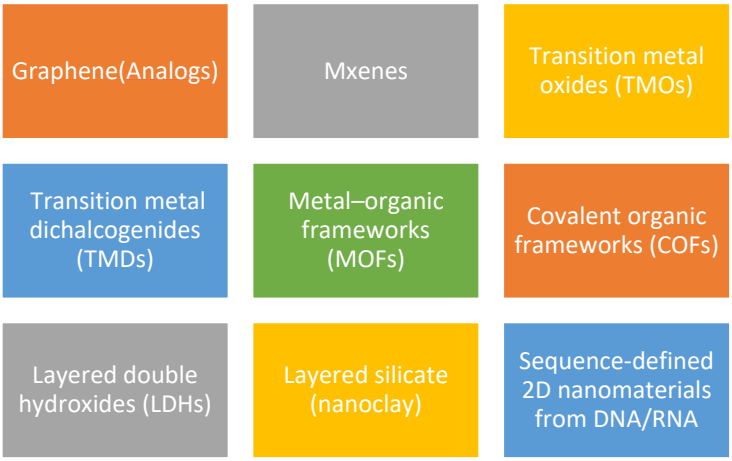

Figure 4. Types of 2D nanomaterials [68]. "Reproduced with permission from Aparna, M. et al., Materials Today; published by Elsevier, 2021".

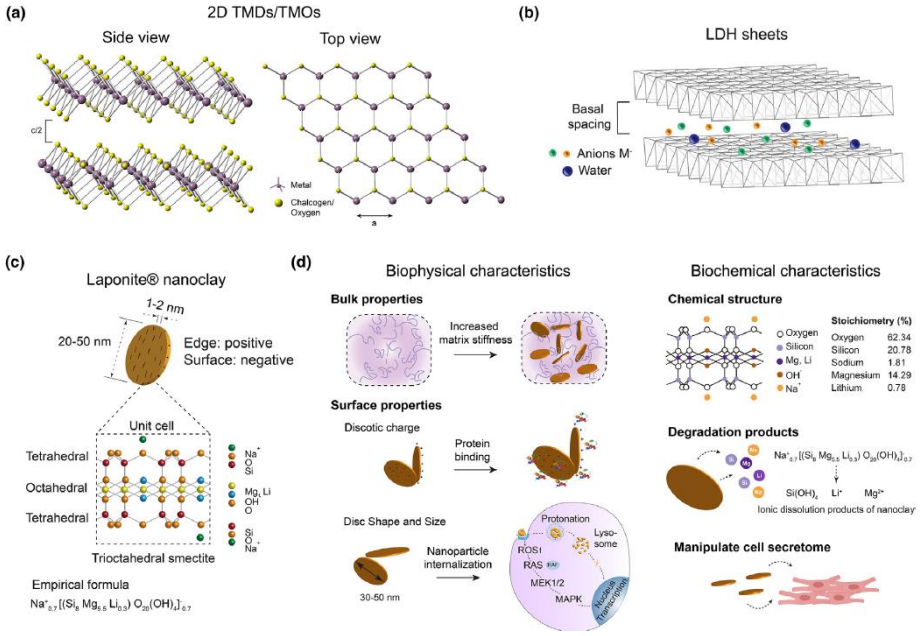

Figure 5. (**a**)The atomistic top and side view of transition metal chalcogenides and oxides; (**b**) illustrative atomic configuration of LDHs; (**c**) atomic configuration of nano clay displaying the crystallographic arrangement of atoms [68]. Reproduced with permission from Aparna, M. et al., Materials Today; published by Elsevier, 2021. (**d**) Schematic representation of biophysical and biochemical characteristics of nanoclay.

TMDs have a metal layer sandwiched between chalcogenides with the general formula MX_2, whereas TMOs are single-layered/multi-layered metal oxides. LDHs have general formula $[M^{2+}{}_{1\_x}M^{3+}{}_x(OH)^2]x^+[A^{P-}{}_{-x/p}]^{x+}\_mH_2O$, where M^{2+} and M^{3+} represent divalent and trivalent metal cations, respectively, at the octahedral positions. 2D Nano clays are silicates of minerals with general formula (Ca, Na, H) (Al, Mg, Fe, Zn)2(Si, Al)$_4O_{10}(OH)_{2-x}H_2O$, where x indicates the amount of water.

7. MXenes

In the ever-expanding world of novel materials, Mxenes are one of the emerging 2D nanomaterials consisting of transition metal carbides, nitrides, or carbonitrides [64]. Mxenes have the general formula M_{n+1} X_n T_x M, are early transition elements, n = 1–3, X is a carbon or nitrogen, and Tx is a surface functional group derived from the MAX phase,

as shown in (Figure 6). With significant polarization loss, high conductivity, and huge chemical active sites, Mxenes are one of the intriguing EMI shielding materials. Ti_3C_2, which is extensively used for EMI shielding applications, crystallizes in the hexagonal P6_3/mmc space group [69]. The local chemical environments are illustrated in (Figure 7) at Ti CSM 4.66 (a), Ti CSM 0.03 (b), and C 0.11 (c) [69].

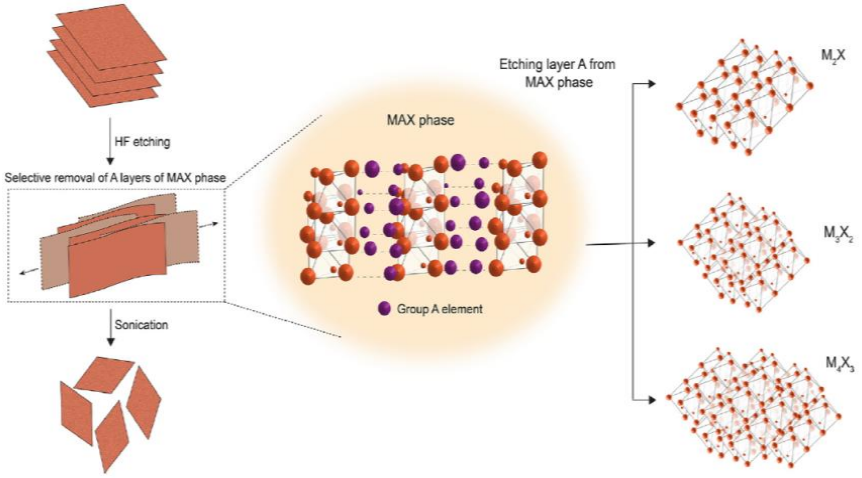

Figure 6. Illustration of Mxene synthesis and different atomic configurations. Adapted from Ref. [68]. Reproduced with permission from Aparna, M. et al., Materials Today; published by Elsevier, 2021.

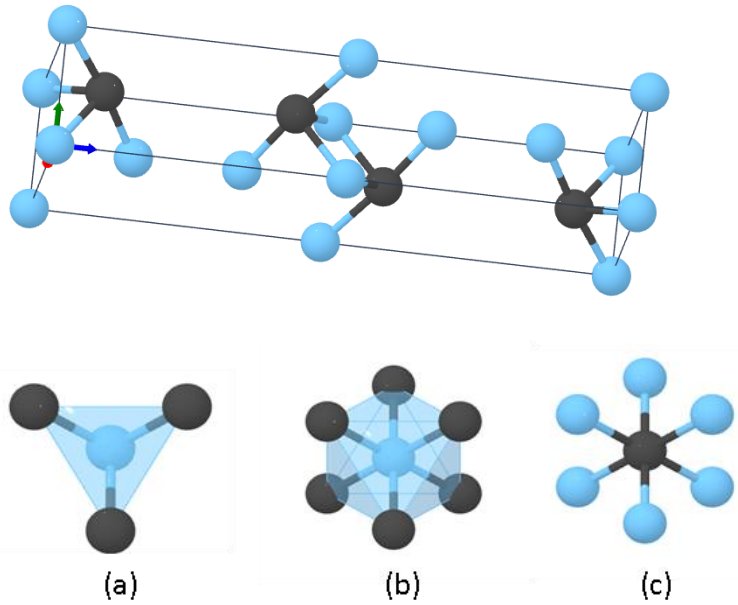

Figure 7. Illustration of titanium carbide crystal structure and the local chemical environments (**a**–**c**) [69].

8. Polymer Nanocomposites

Contrary to the conventional micron-filled composites, these unique nanofillers often modify the properties of the polymer matrix at the same time, bestowing new functionality because of their chemical composition and their nano dimensions. The uniqueness of polymer nanocomposites is rendered by nanofillers which possess small defects, critical length scale (size), and exceptionally large interfacial areas. Defects are structural imperfections; in essence, the real crystal is always idealistic, and crystal imperfections are pragmatic. Basically, there are three kinds of imperfections that can materialize in crystals: point defects, line defects, and plane defects [70] The interaction zone encompassing the filler alters the characteristics of these hybrid materials. Metal or metal oxide polymer nanocomposites (PNCs) are intriguing on account of the aggregation of nanomaterials of

metal and their oxides, layered silicates, semiconductors, graphene, and graphene oxide, which are distributed in the pristine polymer, offering fascinating properties. Ideally, the size of such array of nanomaterials is roughly 1–10 nm. The characteristic properties of these hybrid materials are indeed due to contributions from both phases, but the compelling augmentation is from the interfacial area [71–84]. By the virtue of the interface, the PNCs has been classified into two groups. In class I, a Van der Waals bond or ionic bond renders cohesion to the whole structure in which organic and inorganic constituents are ingrained. In class II materials, the cogent covalent bonds link the two phases [85]. The lamellar nanocomposites exhibit better understanding of interphase interactions between the phases in polymer nanocomposites in which interface interactions between the two phases are magnified. On the basis of structural morphology, lamellar composites are grouped into (a) encapsulated, (b) intercalated, and (c) exfoliated.

In intercalated composites, the polymer chains reorganize with the inorganic layers into a resolute configuration and have an explicit number of polymer layers in the interlayer space. Exfoliated nanocomposites exhibit singular sheets draped within the confines of the polymer network with separation more than 10 nm. The disposition and attributes of the polymer nanocomposites rely upon diverse components such as the structure of the pristine polymer, the nature and quantity of functional groups, and methods of confinement.

9. 2D Nanomaterials-Based Polymer Nanocomposites

To realize adequate electromagnetic shielding globally, scientists have made use of various approaches by using conductive polymers, metals, carbonaceous materials, and metal nanoparticles. Innumerable polymers, including polymethyl methacrylate (PMMA), polystyrene (PS), epoxy resin, polypyrrole (PPY), polyurethane (PU), polylactic acid (PLA), polycarbonate, polyvinyl alcohol (PVA), polyaniline (PANI), and polyvinylidene difluoride (PVDF) are used as the host macromolecular matrix or as blends. The combination offers different structural configurations such as layered structures, aerogels, and foams. The impedance mismatch is one of the predominant criteria for EMI shielding [86], and this is achieved by enhancing the electrical conductivity of the matrix [87]. Due to the high specific area, the availability of surface atoms and surface groups (Figure 8) increases manifold, which in turn provides greater surface energy. With significant polarization loss, high conductivity, and huge chemical active sites, 2D nanomaterials are one of the intriguing EMI shielding materials (Figure 9).

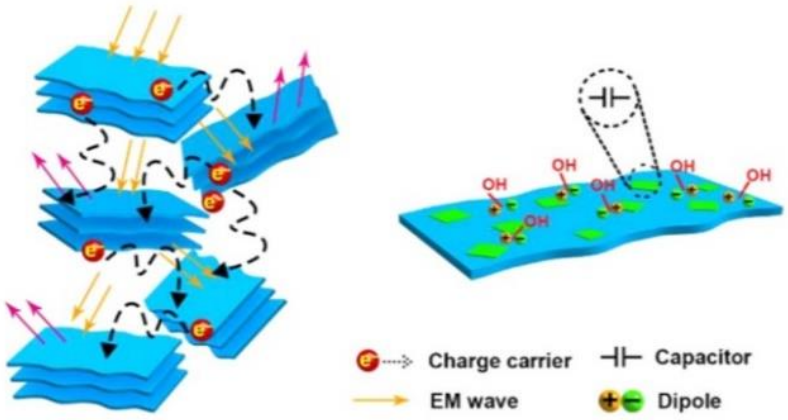

Figure 8. Pictorial representation of EM attenuation for Mxenes [88]. Reproduced with permission from Han, M., et al., Applied Materials Interfaces; published by American Chemical Society, 2016.

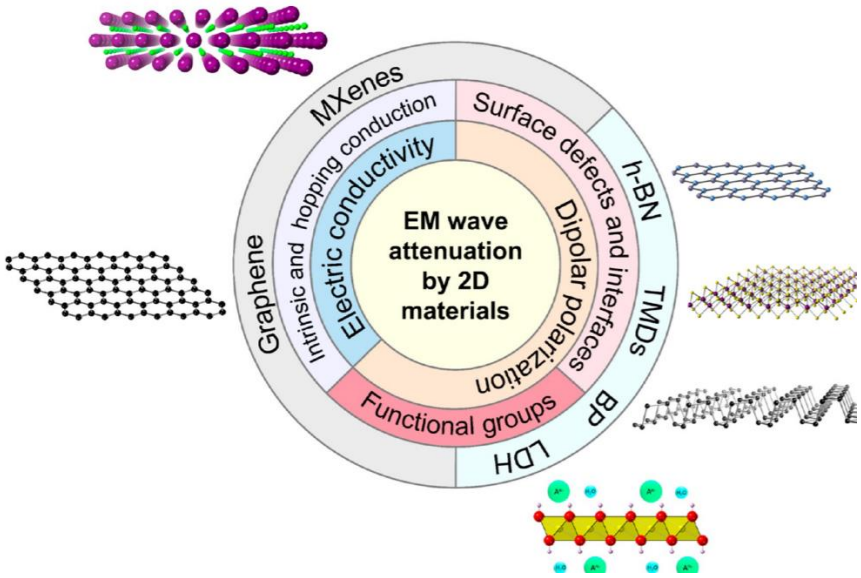

Figure 9. Illustrative representation of various factors impacting the EMI SE of 2D nanomaterials [89]. Reproduced with permission from Filipa, M., et al., ACS Applied Electronic Materials; published by American Chemical Society, 2020.

There was a substantial increase in shielding effectiveness (SE) from 1 dB to 14 dB when graphene nanosheets were dispersed in thermoplastic polyurethane (TPU) [90], whereas graphene/polydimethylsiloxane (PDMS) nanocomposites showed stable shielding effectiveness [91]. The graphene nanosheets dispersed in polyethylene (UHMW) displayed 33% (SE) [92]. On the other hand, (SE) greater than 40 dB (SE) was observed with graphene nanoplatelets and PLA nanocomposites [93]. The graphene nanoplatelets in polyester showed a SE of 27 dB [94], and the correlation studies of the experimental and numerical simulation of graphene in glass/epoxy fiber were in good agreement with SE −27 dB to −31 dB [95]. In another study PVA/MWCNTs/graphene nanosheets composites exhibited SE of (−1.90 dB to −23.1 dB) with greater synergy on the addition of MWCNTS [96]; all the mentioned SE values are at different frequency ranges. The hybrid composites PANI/PVA/few-layered graphene [97] were explored as an alternating promising framework for EMI shielding with a significant increase in (SE) and mechanical properties. The polymer blend of polyvinyl chloride/polyaniline/graphene nanoplatelets displayed SE of 51 dB, and the surface morphology and the SE (due to absorption, reflection and total effect) of these blends with different weight percentage composition is displayed in (Figures 10 and 11). However, the emergence of Mxenes as a potential candidate for EMI shielding with around 2000 publications and 8×10^4 citations in 2021 [98] has changed the dynamics of the domain. The aramid nanofiber/Mxene composite had an SE of 40.6 dB [99]. $Ti3C_2T_x$/calcium alginate films presented a shielding effectiveness of 54.3 dB [100], and in another study cellulose nanofiber/boron nitride nanosheets and Mxene films had an exceptional SE of 60 dB [101]. The elastomer/Mxene composite had an SE of 49 dB in the X-band [102] and polyurethane/Mxene/silver nanowire composites had the transparency for flexible electronics with reasonable SE [103]. The hybrid composite of Mxenes/poly aniline–poly para-aminophenol/poly-pyrrole/poly-thiophene showed 99% SE [104]. The aerogel of polyimide/Mxenes exhibited outstanding microwave absorption with SE of −45.4 dB [105] and MXene/polypropylene (PP) had a SE of 60 dB in the X-band [106]. The Mxene/PMMA/rGO nanocomposites had SE in the range of 28–61 dB [107]. PLA/CNTs/Mxenes had shown SE of 39.6 dB with varying concentrations of the fillers [108]. Lastly, the significant electronic and electrochemical properties [109,110] of the Mxenes makes it one of the potential functional EMI shielding material.

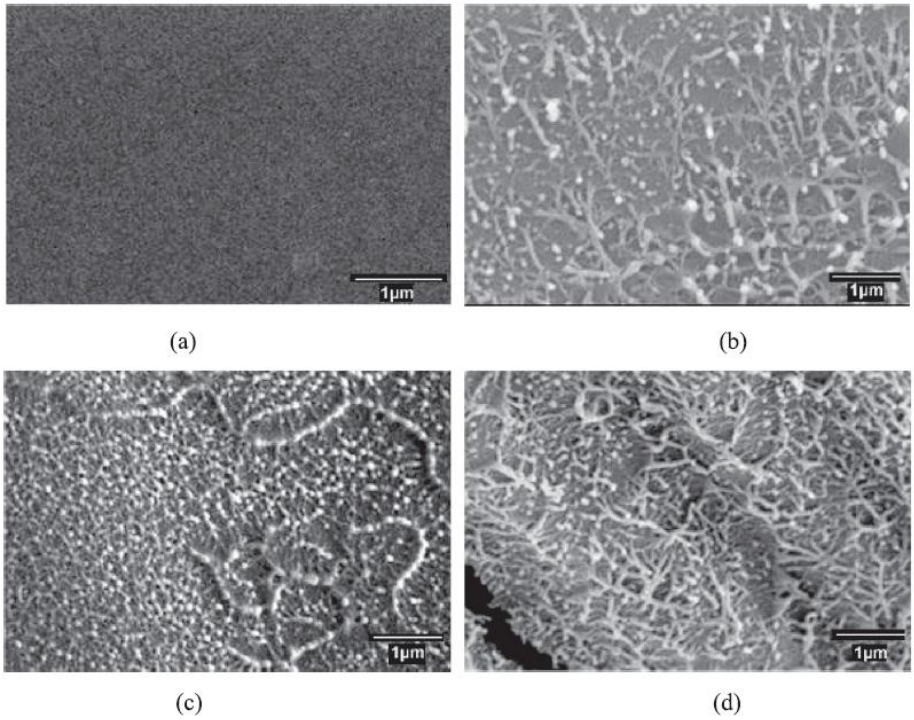

Figure 10. SEM images of PANI/PVC/GNPs [111]. (**a**) PVC only (**b**) PVC/PANI-15 (**c**) PVC/PANI-15/GNP-1 (**d**) PVC/PANI-15/GNP-5. Reproduced with permission from Shakir, M.F., Results in Physics; published by Elsevier, 2019.

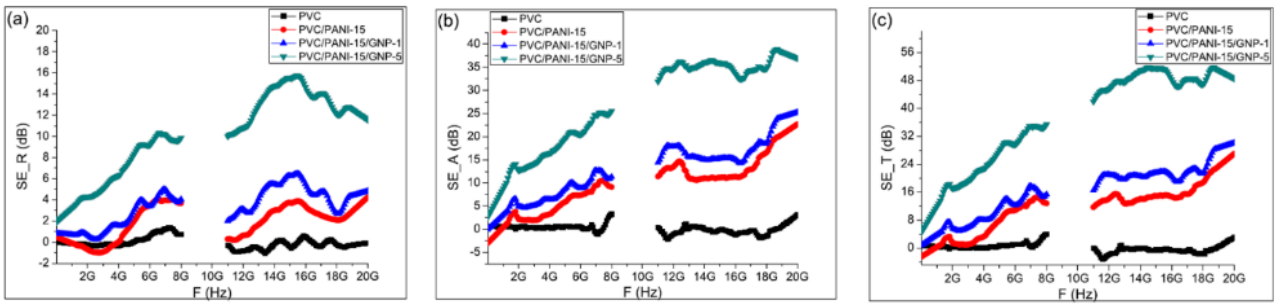

Figure 11. SE of PANI/PVC/GNPs for different weight percentage loading (**a**) reflection (**b**) Absorption and (**c**) total effect of hybrid polymer composites in a frequency 10 MHz–20 GHz [111]. Reproduced with permission from Shakir, M.F., Results in Physics; published by Elsevier, 2019.

The Graphene nanoplatelets (GnP) [112] with different volume fractions when reinforced in the high-density polyethylene (HDPE) matrix in the form of solid and foam nanocomposites demonstrated higher shielding effectiveness in the foamed structure as shown in Figure 12. Figure 12 depicts the shielding mechanism in the HDPE -GnP nanocomposites.

Interestingly, the Graphene—poly(methyl methacrylate) (PMMA) nanolaminates [113] exhibited EMI SE of 60 dB in the THz range (Figure 13), the optimum graphene volume fraction and the thickness studies revealed the absorption mechanism was solely responsible for EMI shielding.

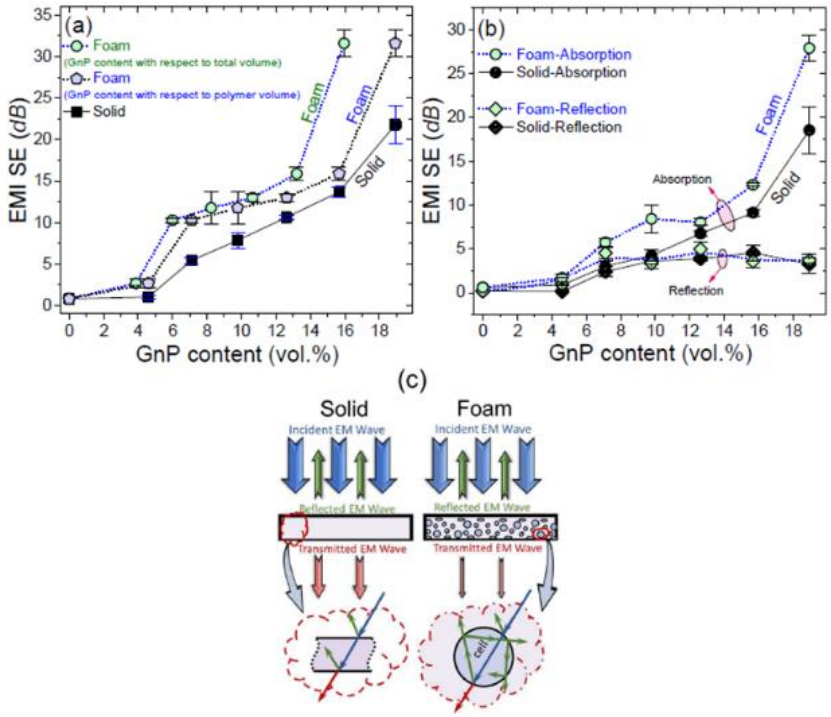

Figure 12. The graphical representation of HDPE-GnP nanocomposite EMI SE as a function of GnP volume fraction with multiple reflection mechanisms (**a**)The K-band EMI SE of the solid and foamed HDPE-GnP composites as a function of their GnP content; (**b**) The contributions of the reflection and absorption mechanisms to the total K-band EMI SE of the solid and foamed HDPE-GnP composites as a function of their GnP content; (**c**) schematic diagrams of the scattering and multiple reflections of the electromagnetic waves [112]. Reproduced with permission from Hamidinejad, M., et al., Aplied Materials; published by American Chemical Society, 2018.

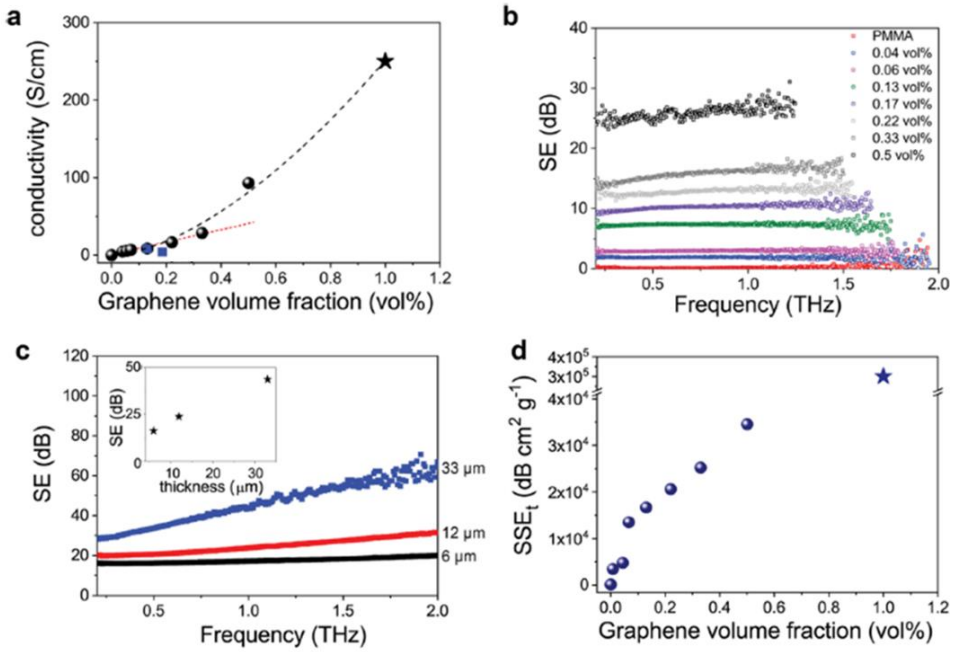

Figure 13. (**a**) Electrical conductivity, (**b**) shielding effectiveness, (**c**) SE with optimum graphene vol%, (**d**) absolute SE [113]. Reproduced with permission from Pavlou, et al., Nature Communications; published by Springer Nature, 2021.

The graphene/MgO/PVA nanocomposites showed an SE of around 20 dB at elevated temperatures, the variation in SE is attributed to the crystallinity of the host matrix of PVA [114]. The absorption and reflection layers of PVDF/Mxenes and PVDF/GnP [115] demonstrated a high EMI SE of 32.6 dB; indeed, the structural configurations of foam/film in the nanocomposites are responsible for effective shielding as depicted in (Figure 14). The hybrid multilayered functional shielding material, namely rGO, MoS_2, Fe_3O_4, and CNTs in PMMA/PVDF/PC polymer matrix [116], was explored in X-band, Ku-band and K-band for total shielding effectiveness; the complex stacking and multilayered structure of the polymer nanocomposite films reiterate that the magnetic nanoparticles as fillers do not significantly alter the EMI SE; on the contrary, plays a pivotal role along with the interfacial polarization loss and defect polarization for EMI SE in polymer nanocomposites. The EM waves attenuation occurs via space charge polarization, orientation polarization, which is a manifestation of interfacial polarization, along with dielectric relaxation and defect polarization [117]. Remarkably, the increase in interfacial area increases the interfacial polarization and the associated loss, which encourages the effective absorption of the incident EM wave [118]. Solitary electron pairs or unsaturated bonds appear at the edge of the vacancy sites, and these defects can be generated as dipole centers to form a strong dipole relaxation effect. The dipoles created under the external electric field can improve the electron migration rate and induce the occurrence of dipole relaxation, thus enhancing the conduction loss and relaxation polarization. Owing to the high specific surface area, 2D nanomaterials are likely to produce enormous amount of dipole moments affecting the dipole polarization [119,120]. The SE of a few PNCs with 2D nanomaterials are listed in Table 2.

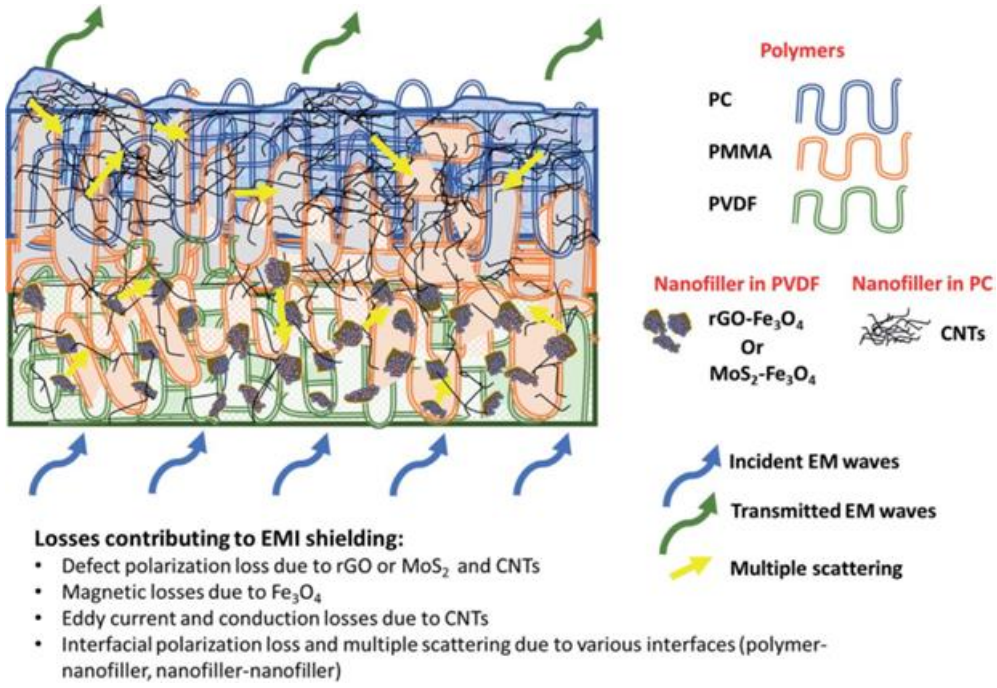

Figure 14. EMI attenuation mechanism in the multilayered architecture of polymer nanocomposites [116]. Reproduced with permission from Sushmitha, K., et al., Nanoscale Advances; published by Royal Society of Chemistry, 2021.

Table 2. EMI shielding performance of various 2D nanomaterials-based polymer nanocomposites.

Materials	Content (wt%)	Thickness, (mm)	EMI SE (dB)	Frequency (GHz)	Ref.
PVDF/GnPs	10	1.5–3	12.4–32.2	26.4–40	[121]
PU/PD/graphene auxetic composite foam	10.8–36.9	0.8–5	upto 57.5	K-band	[122]
CNT/h-BN/rubber composite	10.7	1.4	22.1	10.3	[123]
MWCNT/graphene/silicone rubber elastomer	3.79	-	42	K-band	[124]
GO/styrene-ethylene/butylene-styrene/ BN/PHDDT)	~40	0.02–4	37.92	8–12	[125]
PS/PANI/MoS_2	0.1–1	0.1	92	100 Hz	[126]
PDMS/Fe_3O_4 intercalated MXene and graphene	11.35	1	77–80	X and K band	[127]
PE/GnP/Graphene black	5–25	3	23–27	8–13	[94]
PP/rGO/$MnFe_2O_4$	10	0.5	71.3	8.2–12.4	[128]
PANI/rGO	40	0.25–0.27	104	0.1 to 10	[129]
FCPs/Zeolite imidazole framework (ZIF 67)		2.5–3.7	(−53 to −38.4)	4.4 to 6.6	[130]
3DGNPs/rGO/Epoxy	0–20.4	3	51	X band	[131]
rGO/Epoxy	0.5–2.0	-	38	0.5 to 5	[132]
PEI/G@Fe_3O_4	1–10	2.5	3–18	X band	[133]
PMMA/Graphene	0.2–1.8	4	13–19	X band	[134]
LM/GNs/CNTs/$Ti_3C_2T_x$	1.65–69.59	1.2–3	5–80	X band	[135]
SA/PDMS/$Ti_3C_2T_x$	62–100	2	9.1–53	X band	[136]
PI/$Ti_3C_2T_x$	0.2–2	0.09–0.21	19–77.4	X band	[137]
PS/$Ti_3C_2T_x$	0.4–2.0	1–2	4–62	X band	[138]

10. Conclusions and Future Perspectives

The overall traits of the polymer nanocomposites are driven by the tangible and influential properties of the host materials. The different functional groups in the polymer matrix, such as amide, ester, alcohol, and carbamate, etc., govern the binding of metal ions or complexes of the fillers with the polymer matrix. The sequence of various mechanisms such as chelation, electrostatic interactions, and reduction reactions, control the dispersion of the metal or metal oxide nanofillers in the host polymer matrix. The metal or metal oxide nanofiller's morphology, size, shape, and diversified functional groups usually pose an uphill task to synthesize and render preferred properties in the polymer nanocomposites. The electrical conductivity of composites is determined by the establishment of conductive networks [139]. The amount of filler at which the conductivity networks are formed in the macromolecular matrix is called the percolation threshold. By adding appropriate fillers and ensuring apt dispersion of the fillers, the percolation threshold can be attained, leading to an increase in EMI shielding in polymer nanocomposites. The density and size of nanoparticles inversely affect the number of particles in polymer nanocomposites at a constant filler concentration [140]; the interfacial area reduces by increasing the size and density of nanoparticles, which will impact the EMI shielding effectiveness [140].

The attributes of a perfect EMI shielding material are tunable absorption frequency, outstanding electrical conductivity, wide bandwidth, apt size/layers, structural configuration, and other capabilities [141]. The distinctive properties of 2D nanomaterials, especially

graphene and Mxenes, have exhibited limitless possibilities in several areas. However, the mechanism of interaction of 2D nanomaterials with polymers and microwave absorption is still evolving; thus, modelling and simulation studies would guide the effective usage of 2D nanomaterials for EMI shielding

In recent years, material technologists have developed thousands of 2D nanomaterials computationally, as well as experimentally novel functional materials to suit the ever-expanding issue of EMI. However, as humankind is going to be more reliant on electronic gadgets and communication devices, EMI shielding and mitigation is essential. The dielectric loss is the vital factor that contributes significantly to microwave absorption; consequently, the magnetic loss ought to be increased. Furthermore, the preferable impedance matching is achieved by incorporating magnetic inorganic materials, which also assist in increasing magnetic loss. The structural design comprising honeycomb morphology would increase microwave absorption. Subsequently, the mechanical stability between the fillers and the host matrix is obtained by using surface functional groups on 2D nanomaterials. Though the processing cost of Mxenes is expensive, the EMI shielding materials with Mxenes demonstrate higher shielding effectiveness compared to graphene-based materials. To counter this issue, the optimization of the structures is necessary. Additionally, synthesizing complex hybrids of graphene-based materials with Mxenes of higher electrical conductivity shielding effectiveness could be enhanced.

While the shielding is due to the reflection and absorption, one can improve the shielding by:

(a) Enhancing the internal path length with the presence of scatterers. The morphology of the scatterers plays a crucial role in the number of scatterers for effective shielding.
(b) Alignment of conducting nano-rods enhances reflection-based shielding while retaining a low number of fillers.
(c) For absorption dominant shielding, the presence of magnetic nanoparticles is desirable. Additionally, surface modification enhances the scattering at the surface thereby reducing the amount of radiation entering the shield.

With the development of porous or layered materials such as carbon nanotubes CNTs, it is possible to form three-dimensional (3-D) structures or multiple layered structures to improve the multiple reflections within the material, thereby enhancing the absorption nature. Impregnating with the scatterers and ferrite absorbers is therefore a unique way of improving the absorption while the surface of the 3D structures may have partial reflection properties. Although 2D nanomaterials are promising emerging materials, there are trivial challenges. The structure-property relationships have to be explored for the fine-tuning of the end applications, and these the ecologically sustainable synthesis methods, which are less expensive with better control parameters, have to be optimized. In the case of EMI shielding, different structural configurations of the 2D nanomaterials, such as metamaterials, foams, etc., which are lightweight, flexible, and cost-effective, need to be fabricated.

Author Contributions: P.K.S. and R.V. and R.P.: methodology and software; R.N. and R.B.: conceptualization, supervision, writing, and editing—original draft; P.B. and A.B.R.: data curation and results analysis; N.A.-Q.: funding acquisition. All authors have read and agreed to the published version of the manuscript.

Funding: This work was supported by Qatar University through a National Capacity Building Program Grant (NCBP), [QUCP-CAM-20/23-463]. Statements made herein are solely the responsibility of the authors.

Data Availability Statement: Data are contained within the article.

Conflicts of Interest: The authors declare no conflict of interest.

References

1. Violette, J.L.N.; White, D.R.J.; Violette, M.F. An Introduction to Electromagnetic Compatibility. In *Electromagnetic Compatibility Handbook*; Springer: Dordrecht, The Netherlands, 1987; pp. 1–12.
2. Jang, J.O.; Park, J.W. Coating Materials for Shielding Electromagnetic Waves. U.S. Patent 6355707 B1, 12 March 2002. Available online: https://patents.google.com/patent/US6355707B1/en,2002 (accessed on 1 December 2022).
3. Schulz, R.; Plantz, V.; Brush, D. Shielding theory and practice. *IEEE Trans. Electromagn. Compat.* **1988**, *30*, 187–201. [CrossRef]
4. Yang, Y.; Gupta, M.C.; Dudley, K.L.; Lawrence, R.W. Conductive Carbon Nanofiber-Polymer Foam Structures. *Adv. Mater.* **2005**, *17*, 1999–2003. [CrossRef]
5. Uiseok, H.; Junyoung, K.; Mina, S.; Bumhee, L.; In-Kyung, P.; Jonghwan, S.; Jae-Do, N. Quantitative Interpretation of Electromagnetic Interference Shielding Efficiency: Is It Really a Wave Absorber or a Reflector? *ACS Omega* **2022**, *7*, 4135–4139.
6. Seung, H.R.; You, K.H.; Suk, J.K.; Taehoon, K.; Byung, M.J.; Sang-Bok, L.; Byeongjin, P. Absorption-dominant, low re-flection EMI shielding materials with integrated metal mesh/TPU/CIP composite. *Chem. Eng. J.* **2022**, *428*, 131167.
7. Kumar, G.S.; Patro, T.U.; Raagulan, K.; Braveenth, R.; Jang, H.J.; Seon Lee, Y.; Yang, C.M.; Mi Kim, B.; Moon, J.J.; Chai, K.Y. Electromagnetic Shielding by MXene-Graphene-PVDF Composite with Hydrophobic, Lightweight and Flexible Graphene Coated Fabric. *Materials* **2018**, *11*, 1803.
8. Xie, P.; Liu, Y.; Feng, M.; Niu, M.; Liu, C.; Wu, N.; Sui, K.; Patil, R.R.; Pan, D.; Guo, Z.; et al. Hierarchically porous Co/C nano-composites for ultralight high-performance microwave absorption. *Adv. Compos. Hybrid Mater.* **2021**, *4*, 173–185. [CrossRef]
9. Wei, S.; Chen, T.; Wang, Q.; Shi, Z.; Li, W.; Chen, S. Metal-organic framework derived hollow CoFe@C composites by the tun-able chemical composition for efficient microwave absorption. *J. Coll. Inter. Sci.* **2021**, *593*, 370–379. [CrossRef]
10. Zhang, Z.; Liu, M.; Ibrahim, M.M.; Haikun, W.; Yan, W.; Yang, L.; Mersal, G.A.M.; Azab, I.H.E.; El-Bahy, S.M.; Huang, M.; et al. Flexible polystyrene/graphene composites with epsilon-near-zero prop-erties. *Adv. Compos. Hybrid Mater.* **2022**, *5*, 1054–1066. [CrossRef]
11. Xie, P.; Shi, Z.; Feng, M.; Sun, K.; Liu, Y.; Yan, K.; Liu, C.; Moussa, T.A.A.; Huang, M.; Meng, S.; et al. Recent advances in radio-frequency negative dielectric metamaterials by designing heterogeneous composites. *Adv. Compos. Hybrid Mater.* **2022**, *5*, 679–695. [CrossRef]
12. Chung, D.D.L. Electromagnetic interference shielding effectiveness of carbon materials. *Carbon* **2001**, *39*, 279–285. [CrossRef]
13. Fan, X.; Guan, J.; Wang, W.; Tong, G. Morphology evolution, magnetic and microwave absorption properties of nano/submicrometre iron particles obtained at different reduced temperatures. *J. Phys. D Appl. Phys.* **2009**, *42*, 075006. [CrossRef]
14. Cao, M.; Song, W.; Hou, Z.; Wen, B.; Yuan, J. The effects of temperature and frequency on the dielectric properties, electro-magnetic interference shielding and microwave-absorption of short carbon fiber/silica composites. *Carbon* **2010**, *48*, 788–796. [CrossRef]
15. Xie, P.; Li, H.; He, B.; Dang, F.; Lin, J.; Fan, R.; Hou, C.; Liu, H.; Zhang, J.; Ma, Y.; et al. Bio-gel derived nickel/carbon nanocom-posites with enhanced microwave absorption. *J. Mater. Chem. C* **2018**, *6*, 8812–8822. [CrossRef]
16. Omana, L.; Chandran, A.; John, R.E.; Wilson, R.; George, K.C.; Unnikrishnan, N.V.; Varghese, S.S.; George, G.; Simon, S.M.; Paul, I. Recent Advances in Polymer Nanocomposites for Electromagnetic Interference Shielding: A Review. *ACS Omega* **2022**, *7*, 25921–25947. [CrossRef]
17. Pai, A.R.; Azeez, N.P.; Thankan, B.; Gopakumar, N.; Jaroszewski, M.; Paoloni, C.; Kalarikkal, N.; Thomas, S. Recent Progress in Electromagnetic Interference Shielding Performance of Porous Polymer Nanocomposites—A Review. *Energies* **2022**, *15*, 3901. [CrossRef]
18. Dar, M.A.; Kotnala, R.K.; Verma, V.; Shah, J.; Siddiqui, W.A.; Alam, M. High Magneto-Crystalline Anisotropic Core–Shell Structured Mn0.5Zn0.5Fe2O4/Polyaniline Nanocomposites Prepared by in Situ Emulsion Polymerization. *J. Phys. Chem.* **2012**, *116*, 5277–5287. [CrossRef]
19. Saini, P.; Choudhary, V.; Singh, B.P.; Mathur, R.B.; Dhawan, S.K. Enhanced microwave absorption behaviour of polyan-iline-CNT/polystyrene blend in 12.4–18.0 GHz Range. *Synth. Met.* **2011**, *161*, 1522–1526. [CrossRef]
20. Choudhary, V.; Dhawan, S.K.; Saini, P. *Polymer Based Nanocomposites for Electromagnetic Interference (EMI) Shielding EM Shielding—Theory and Development of New Materials*; Jaroszewski, M., Ziaja, J., Eds.; Research Signpost: Thiruvananthapuram, India, 2012; pp. 1–29. ISBN 978-81-308-0499-6.
21. Khan, R.; Khan, Z.M.; Bin Aqeel, H.; Javed, S.; Shafqat, A.; Qazi, I.; Basit, M.A.; Jan, R. 2D nanosheets and composites for EMI shielding analysis. *Sci. Rep.* **2020**, *10*, 21550. [CrossRef]
22. Chung, D.D.L. Materials for electromagnetic interference shielding. *Mater. Chem. Phys.* **2020**, *255*, 123587. [CrossRef]
23. Cui, T.J.; Smith, D.R.; Liu, R. *Metamaterials: Theory, Design, and Applications*; Springer: Berlin/Heidelberg, Germany, 2010; ISBN 9781441905727.
24. Engheta, N.; Ziolkowski, R.W. *Metamaterials: Physics and Engineering Explorations*; Wiley IEEE Press: New York, NY, USA, 2006; pp. 3–30, 37, 143–150, 215–234, 240–256.
25. Saïd, Z.; Ari Sihvola, A.; Vinogradov, A.P. *Metamaterials and Plasmonics: Fundamentals, Modelling, Applications*; Springer: New York, NY, USA, 2008; Volume 106, pp. 3–10.
26. Smith, D.R.; Pendry, J.B. Homogenization of metamaterials by field averaging. *J. Opt. Soc. Am. B* **2006**, *23*, 321. [CrossRef]
27. Davi, B.B. *Metamaterial Inspired Improved Antenna and Circuits*; Electromagnetism; Télécom ParisTech: Paris, France, 2010; pp. 19–27, English. ffpastel-00749642f, UFRN.
28. Engheta, N.; Ziolkowski, R.W. Antennas Propagation, Special Issue on Metamaterials. *IEEE Trans.* **2003**, *51*, 2546–2750.

29. Engheta, N.; Ziolkowski, R. A positive future for double-negative metamaterials. *IEEE Trans. Microw. Theory Technol.* **2005**, *53*, 1535–1556. [CrossRef]
30. Buriak, I.; Zhurba, V.O.; Vorobjov, G.S.; Kulizhko, V.R.; Kononov, O.; Rybalko, O. Metamaterials: Theory, Classification and Application Strategies (Review). *J. Nano-Electron. Phys.* **2016**, *8*, 04088. [CrossRef]
31. Depine, R.A.; Lakhtakia, A. A new condition to identify isotropic dielectric-magnetic materials displaying negative phase velocity. *Microw. Opt. Technol. Lett.* **2004**, *41*, 315–316. [CrossRef]
32. Voznesenskaya, A.; Kabanova, D. Analysis of Ray Tracing through Optical Systems with Metamaterial Elements. *Sci. Technol. J. Inf.* **2012**, *81*, 5–10.
33. Yasser, Z.; Kyong, Y.R. A simple methodology to predict the tunnelling conductivity of polymer/CNT nanocomposites by the roles of tunneling distance, interphase and CNT waviness. *RSC Adv.* **2017**, *7*, 34912.
34. Razavi, R.; Zare, Y.; Rhee, K.Y. A two-step model for the tunneling conductivity of polymer carbon nanotube nanocomposites assuming the conduction of interphase regions. *RSC Adv.* **2017**, *7*, 50225–50233. [CrossRef]
35. Kovacs, J.Z.; Velagala, B.S.; Schulte, K.; Bauhofer, W. Two percolation thresholds in carbon nanotube epoxy composites. *Compos. Sci. Technol.* **2007**, *67*, 922–928. [CrossRef]
36. Kumar, G.S.; Patro, T.U. Efficient electromagnetic interference shielding and radar absorbing properties of ultrathin and flexible polymer-carbon nanotube composite films. *Mater. Res. Express* **2018**, *5*, 115304. [CrossRef]
37. Hoang, A.S. Electrical conductivity and electromagnetic interference shielding characteristics of multiwalled carbon nanotube filled polyurethane composite films. *Adv. Nat. Sci. Nanosci. Nanotechnol.* **2011**, *2*, 025007. [CrossRef]
38. Hoang, A.S.; Nguyen, H.N.; Bui, H.T.; Tuan, A.T.; Anh, D.V.; Nguyen, B.; Van, B.N. Carbon nanotubes materials and their application to guarantee safety from exposure to electromagnetic fields. *Adv. Nat. Sci. Nanosci. Nanotechnol.* **2013**, *4*, 025012. [CrossRef]
39. Verma, R.; Rathod, M.J.; Goyal, R.K. High electromagnetic interference shielding of poly(ether-sulfone)/multi-walled carbon nanotube nanocomposites fabricated by an eco-friendly route. *Nanotechnology* **2020**, *31*, 385702. [CrossRef] [PubMed]
40. Bertolini, M.C.; Ramoa, S.D.A.S.; Merlini, C.; Barra, G.M.O.; Soares, B.G.; Pegoretti, A. Hybrid Composites Based on Thermoplastic Polyurethane with a Mixture of Carbon Nanotubes and Carbon Black Modified with Polypyrrole for Electromagnetic Shielding. *Front. Mater.* **2020**, *7*, 174. [CrossRef]
41. Ramírez-Herrera, C.A.; Gonzalez, H.; de la Torre, F.; Benitez, L.; Cabañas-Moreno, J.G.; Lozano, K. Electrical Properties and Electromagnetic Interference Shielding Effectiveness of Interlayered Systems Composed by Carbon Nanotube Filled Carbon Nanofiber Mats and Polymer Composites. *Nanomaterials* **2019**, *9*, 238. [CrossRef]
42. Yanju, L.; Di, S.; Chunxia, W.; Jinsong, L. EMI shielding performance of nanocomposites with MWCNTs, nanosized Fe3O4 and Fe. *Compos. B Eng.* **2014**, *63*, 34–40.
43. Li, J.; Lu, W.; Suhr, J.; Chen, H.; Xiao, J.Q.; Chou, T.-W. Superb electromagnetic wave-absorbing composites based on large-scale graphene and carbon nanotube films. *Sci. Rep.* **2017**, *7*, 2349. [CrossRef]
44. Zhengkang, X.; Aili, J.; Xulin, Y.; Yang, X.; Feng, W.; Wang, P.; Li, K.; Lei, W.; He, H.; Tian, Y.; et al. Controllable modification of helical carbon nanotubes for high-performance microwave absorption. *Nanotechnol. Rev.* **2021**, *10*, 671–679.
45. Zuomin, L.; Dingkun, T.; Xuebin, L.; Jianhong, W.; Krishnamoorthy, R.; Tao, Z.; Yougen, H.; Pengli, Z.; Rong, S.; Ching-Ping, W. Electrically conductive gradient structure design of thermoplastic polyurethane composite foams for efficient electro-magnetic interference shielding and ultra-low microwave reflectivity. *Chem. Eng. J.* **2021**, *424*, 130365.
46. Jianming, Y.; Xia, L.; Gui, W.; Wang, J.; Jia, C.; Wanyu, T.; Tengfei, W.; Guangxian, L. Fabrication of lightweight and flexible silicon rubber foams with ultra-efficient electromagnetic interference shielding and adjustable low reflectivity. *J. Mater. Chem. C* **2020**, *8*, 147–157.
47. Shu, Z.; Qingya, Z.; Mengya, W.; Jackson, D.; Zhe, Q.; Yuchi, F.; Meifang, Z.; Changhuai, Y. Modulating electromagnetic interference shielding performance of ultra-lightweight composite foams through shape memory function. *Compos. B Eng.* **2021**, *204*, 108497.
48. Dongwei, L.; Zichao, M.; Binghao, L.; Leilei, Y.; Zhongfu, H.; Hai, Z.; Zikang, T.; Xuchun, G. Flexible, lightweight carbon nano-tube sponges and composites for high-performance electromagnetic interference shielding. *Carbon* **2018**, *133*, 457–463.
49. Wang, Y.Y.; Zhou, Z.H.; Zhou, C.G.; Sun, W.J.; Gao, J.F.; Dai, K.; Yan, D.X.; Li, Z.M. Lightweight and Robust Carbon Nanotube/Polyimide Foam for Efficient and Heat-Resistant Electromagnetic Interference Shielding and Microwave Absorption. *ACS Appl. Mater. Interfaces* **2020**, *12*, 8704–8712. [CrossRef] [PubMed]
50. Wu, T.; Mei, X.; Liang, L.; Xin, P.; Guibin, W.; Shuling, Z. Structure-function integrated poly (aryl ether ketone)-grafted MWCNTs/poly (ether ether ketone) composites with low percolation threshold of both conductivity and electromagnetic shielding. *Compos. Sci. Technol.* **2022**, *217*, 109032. [CrossRef]
51. Wang, Y.Y.; Yang, S.; Sun, W.-J.; Dai, K.; Yan, D.X.; Li, Z.M. Highly enhanced microwave absorption for carbon nano-tube/barium ferrite composite with ultra-low carbon nanotube loading. *J. Mater. Sci. Technol.* **2022**, *102*, 115–122. [CrossRef]
52. Anjaneyalu, A.M.; Zeraati, A.S.; Sundararaj, U. Enhanced electromagnetic interference shielding effectiveness of hybrid fillers by segregated structure. *AIP Conf. Proc.* **2019**, *2065*, 040009. [CrossRef]
53. Wang, M.; Zhang, Y.; Dong, C.; Chen, G.; Guan, H. Preparation and electromagnetic shielding effectiveness of cobalt ferrite nanoparticles/carbon nanotubes composites. *Nanomater. Nanotechnol.* **2019**, *9*, 1–7. [CrossRef]

54. Li, G.; Sheng, L.; Liming, Y.L.; An, K.; Ren, W.; Zhao, X. Electromagnetic and microwave absorption properties of sin-gle-walled carbon nanotubes and CoFe2O4 nanocomposites. *Mater. Sci. Eng. B* **2015**, *193*, 153–159. [CrossRef]
55. Phan, C.H.; Mariatti, M.; Koh, Y.H. Electromagnetic interference shielding performance of epoxy composites filled with multiwalled carbon nanotubes/manganese zinc ferrite hybrid fillers. *J. Magn. Magn. Mater.* **2016**, *401*, 472–478. [CrossRef]
56. Rosdi, N.; Azis, R.S.; Ismail, I.; Mokhtar, N.; Zulkimi, M.M.M.; Mustaffa, M.I. Structural, microstructural, magnetic and electromagnetic absorption properties of spiraled multiwalled carbon nanotubes/barium hexaferrite (MWCNTs/BaFe12O19) hy-brid. *Sci. Rep.* **2021**, *11*, 15982. [CrossRef]
57. Yu, L.; Zhu, Y.; Qian, C.; Fu, Q.; Zhao, Y.; Fu, Y. Nanostructured Barium Titanate/Carbon Nanotubes Incorporated Polyaniline as Synergistic Electromagnetic Wave Absorbers. *J. Nanomater.* **2016**, *2016*, 6032307. [CrossRef]
58. Al-Saleh, M.H.; Saadeh, W.H.; Sundararaj, U. EMI shielding effectiveness of carbon based nanostructured polymeric materials: A comparative study. *Carbon* **2013**, *60*, 146–156. [CrossRef]
59. Kuang, T.; Chang, L.; Chen, F.; Sheng, Y.; Fu, D.; Peng, X. Facile preparation oflightweight high-strength biodegradable poly-mer/multi-walled carbon nanotubes nanocomposite foams for electromagnetic interference shielding. *Carbon* **2016**, *4*, 052.
60. Sainia, P.; Choudhary, V.; Singh, B.P.; Mathur, R.B.; Dhawan, S.K. Polyaniline–MWCNT nanocomposites for microwave absorption and EMI shielding. *Mat. Chem. Phy.* **2009**, *113*, 919–926. [CrossRef]
61. Tan, C.; Cao, X.; Wu, X.-J.; He, Q.; Yang, J.; Zhang, X.; Chen, J.; Zhao, W.; Han, S.; Nam, G.-H.; et al. Recent Advances in Ultrathin Two-Dimensional Nanomaterials. *Chem. Rev.* **2017**, *117*, 6225–6331. [CrossRef]
62. Low, J.; Cao, S.; Yu, J.; Wageh, S. Two-dimensional layered composite photocatalysts. *Chem. Commun.* **2014**, *50*, 10768–10777. [CrossRef]
63. Geim, A.K.; Novoselov, K.S. The rise of graphene. *Nat. Mater.* **2007**, *6*, 183–191. [CrossRef]
64. Fiori, G.; Bonaccorso, F.; Iannaccone, G.; Palacios, T.; Neumaier, D.; Seabaugh, A.; Banerjee, S.K.; Colombo, L. Electronics based on two-dimensional materials. *Nat. Nanotechnol.* **2014**, *9*, 768–779, Erratum in *Nat. Nanotechnol.* **2014**, *9*, 1063. [CrossRef]
65. Sun, Y.; Gao, S.; Xie, Y. Atomically-thick two-dimensional crystals: Electronic structure regulation and energy device con-struction. *Chem. Soc. Rev.* **2014**, *43*, 530–546. [CrossRef]
66. Zhang, J.; Chen, Y.; Wang, X. Two-dimensional covalent carbon nitride nanosheets: Synthesis, functionalization, and applications. *Energy Environ. Sci.* **2015**, *8*, 3092–3108. [CrossRef]
67. Naguib, M.; Mochalin, V.N.; Barsoum, M.W.; Gogotsi, Y. 25th Anniversary Article: MXenes: A New Family of Two-Dimensional Materials. *Adv. Mater.* **2015**, *26*, 992–1005. [CrossRef]
68. Aparna, M.; Giriraj, L.; Kaivalya, A.; Brokesh, A.; Gaharwar, A.K. Emerging 2D nanomaterials for biomedical applications. *Mat. Today* **2021**, *50*, 276–302.
69. Jain, A.; Ong, S.P.; Hautier, G.; Chen, W.; Richards, W.D.; Dacek, S.; Cholia, S.; Gunter, D.; Skinner, D.; Ceder, G.; et al. The Materials Project: A materials genome approach to accelerating materials innovation. *APL Mater.* **2013**, *1*, 011002. [CrossRef]
70. Jurgen, S.; Stefan, K.E. Perspectives on the Theory of Defects. *Front. Mater.* **2018**, *5*, 70. [CrossRef]
71. Huang, W.; Hu, L.; Tang, Y.; Xie, Z.; Zhang, H. Recent Advances in Functional 2D MXene-Based Nanostructures for Next-Generation Devices. *Adv. Funct. Mater.* **2020**, *30*, 2005223. [CrossRef]
72. Sankaran, S.; Deshmukh, K.; Ahamed, M.B.; Pasha, S.K. Recent advances in electromagnetic interference shielding properties of metal and carbon filler reinforced flexible polymer composites: A review. *Compos. Part A Appl. Sci. Manuf.* **2018**, *114*, 49–71. [CrossRef]
73. Mukherjee, M.; Datta, A.; Chakravorty, D. Electrical resistivity of nanocrystalline PbS grown in a polymer matrix. *Appl. Phys. Lett.* **1994**, *64*, 1159–1161. [CrossRef]
74. Chen, T.K.; Tien, Y.I.; Wei, K.H. Synthesis and characterization of novel segmented polyurethane/clay nanocomposites. *Polymer* **2000**, *41*, 1345–1353. [CrossRef]
75. Wei, Y.; Zhang, X.; Song, Y.; Han, B.; Hu, X.; Wang, X.; Lin, Y.; Deng, X. Magnetic biodegradable Fe3O4/CS/PVA nanofibrous membranes for bone regeneration. *Biomed. Mater.* **2011**, *6*, 055008. [CrossRef]
76. Kharazmi, A.; Saion, E.; Faraji, N.; Soltani, N.; Dehzangi, A. Optical Properties of CdS/PVA Nanocomposite Films Synthesized using the Gamma-Irradiation-Induced Method. *Chin. Phys. Lett.* **2013**, *30*, 057803. [CrossRef]
77. Chen, J.; Beake, B.D.; Bell, Y.; Yalan, T.; Fengge, G. Effects in nylon 6-clay nanocomposites and Probing polymer chain con-straint and synergistic effects in nylon 6- clay nanocomposites and nylon 6-silica flake sub-micro composites with nano me-chanics. *Nanocomposites* **2016**, *1*, 185–194. [CrossRef]
78. Abulyazied, D.E.; Mokhtar, S.M.; Motawie, A.M. Nanoindentation Behaviorand Physical Properties of Polyvinyl Chloride/Styrene co-maleic anhydride blend reinforced by Nano-Bentonite. *IOSR-JAC* **2014**, *7*, 32–44.
79. El-kader, F.H.A.; Hakeem, N.A.; Elashmawi, I.S.; Ismail, A.M. Structural, Optical and Thermal Characterization of ZnO Nanoparticles Doped in PEO / PVA Blend Films. *Aust. J. Basic Appl. Sci.* **2013**, *7*, 608–619.
80. Okada, A.; Usuki, A. Twenty years of polymer-clay nanocomposites. *Macromol. Mater. Eng.* **2006**, *291*, 449–1476. [CrossRef]
81. Winey, K.I.; Vaia, R.A. Polymer nanocomposites. *Mater. Res. Bull.* **2007**, *32*, 314–322. [CrossRef]
82. Krishnamoorti, R.; Vaia, R.A. Polymer nanocomposites. *J. Polym. Sci. B Polym. Phys.* **2007**, *45*, 3252–3256. [CrossRef]
83. Balazs, A.C.; Emrick, T.; Russell, T.P. Nanoparticle Polymer Composites: Where Two Small Worlds Meet. *Science* **2006**, *314*, 1107–1110. [CrossRef]
84. Schaefer, D.W.; Justice, R.S. How nano are nanocomposite? *Macromolecules* **2007**, *40*, 8501–8517. [CrossRef]

85. Julia, B.; Popall, M. Applications of hybrid organic—Inorganic nanocomposites. *J. Mater. Chem.* **2005**, *15*, 3559–3592.
86. Qin, M.; Zhang, L.; Wu, H. Dielectric Loss Mechanism in Electromagnetic Wave Absorbing Materials. *Adv. Sci.* **2022**, *9*, e2105553. [CrossRef] [PubMed]
87. Lecocq, H.; Garois, N.; Lhost, O.; Girard, P.-F.; Cassagnau, P.; Serghei, A. Polypropylene/carbon nanotubes composite materials with enhanced electromagnetic interference shielding performance: Properties and modelling. *Comp. Part B Eng.* **2020**, *189*, 107866. [CrossRef]
88. Han, M.; Yin, X.; Wu, H.; Hou, Z.; Song, C.; Li, X.; Zhang, L.; Cheng, L. Ti_3C_2 MXenes with Modified Surface for High-Performance Electromagnetic Absorption and Shielding in the X-Band. *ACS Appl. Mater. Interfaces* **2016**, *8*, 21011–21019. [CrossRef] [PubMed]
89. Filipa, M.; Rui Gusmão, O. Recent Advances in the Electromagnetic Interference Shielding of 2D Materials beyond Graphene. *ACS Appl. Elect. Mat.* **2020**, *2*, 3048–3071.
90. Jan, R.; Habib, A.; Aftab Akram, M.; Ahmad, I.; Shah, A.; Sadiq, M.; Hussain, A. Flexible, thin films of graphene-polymer composites for EMI shielding. *Mat. Res. Exp.* **2017**, *4*, 035605. [CrossRef]
91. Zhenyu, W.; Wenzhen, Y.; Rui, L.; Zhang, X.; Nie, H.; Liu, Y. Highly stretchable graphene/polydimethylsiloxane composite lattices with tailored structure for strain-tolerant EMI shielding performance. *Compos. Sci. Technol.* **2021**, *206*, 108652.
92. Al-Saleh, M.H. Electrical and electromagnetic interference shielding characteristics of GNP/UHMWPE composites. *J. Phys. D Appl. Phys.* **2016**, *49*, 195302. [CrossRef]
93. Zeranska-Chudek, K.; Wróblewska, A.; Kowalczyk, S.; Plichta, A.; Zdrojek, M. Graphene Infused Ecological Polymer Composites for Electromagnetic Interference Shielding and Heat Management Applications. *Materials* **2021**, *14*, 2856. [CrossRef] [PubMed]
94. Madinehei, M.; Kuester, S.; Kaydanova, T.; Moghimian, N.; David, É. Influence of Graphene Nanoplatelet Lateral Size on the Electrical Conductivity and Electromagnetic Interference Shielding Performance of Polyester Nanocomposites. *Polymers* **2021**, *13*, 2567. [CrossRef] [PubMed]
95. Santhosi, B.; Ramji, K.; Rao, N.M. Design and development of polymeric nanocomposite reinforced with graphene for effective EMI shielding in X-band. *Phys. B Condens. Matter* **2020**, *586*, 412144. [CrossRef]
96. Lin, J.-H.; Lin, Z.-I.; Pan, Y.-J.; Chen, C.H.; Lin, C.; Chen-Hung, H.; Lou, C.W. Improvement in Mechanical Properties and Electromagnetic Interference Shielding Effectiveness of PVA-Based Composites: Synergistic Effect Between Graphene Nano-Sheets and Multi-Walled Carbon Nanotubes. *Macromol. Mater. Eng.* **2016**, *301*, 199–211. [CrossRef]
97. Khan, M.; Khan, A.N.; Saboor, A.; Gul, I.H. Investigating mechanical, dielectric, and electromagnetic interference shielding properties of polymer blends and three component hybrid composites based on polyvinyl alcohol, polyaniline, and few layer graphene. *Polym. Compos.* **2017**, *39*, 3686–3695. [CrossRef]
98. Naguib, M.; Barsoum, M.W.; Gogotsi, Y. Ten Years of Progress in the Synthesis and Development of MXenes. *Adv. Mater.* **2021**, *33*, 2103393. [CrossRef]
99. Weng, C.; Xing, T.; Jin, H.; Wang, G.; Dai, Z.; Pei, Y.; Liu, L.; Zhang, Z. Mechanically robust ANF/MXene composite films with tunable electromagnetic interference shielding performance. *Compos. Part A Appl. Sci. Manuf.* **2020**, *135*, 105927. [CrossRef]
100. Zhou, Z.; Liu, J.; Zhang, X.; Tian, D.; Zhan, Z.; Lu, C. Ultrathin MXene/Calcium Alginate Aerogel Film for High-Performance Electromagnetic Interference Shielding. *Adv. Mater. Interfaces* **2019**, *6*, 1802040. [CrossRef]
101. Ying, S.; Youxin, J.; Jingwen, D.; Gui, Y.; Zhang, X.; Su, F.; Feng, Y.; Liu, C. Sandwiched cellulose nanofiber /boron nitride nanosheet /Ti3C2Tx MXene composite film with high electromagnetic shielding and thermal conductivity yet insulation per-formance. *Compos. Sci. Technol.* **2021**, *214*, 108974.
102. Aakyiir, M.; Kingu, M.-A.S.; Araby, S. Stretchable, mechanically resilient, and high electromagnetic shielding polymer/MXene nanocomposites. *J. Appl. Polym. Sci.* **2021**, *138*, e50509. [CrossRef]
103. Shengchi, B.; Xingzhong, G.; Xuyang, Z.; Parchment, D.; Anasori, B.; Koo, C.M.; Friedman, G.; Gogotsi, Y. Ti3C2Tx MXene-AgNW composite flexible transparent conductive films for EMI shielding. *Compos. Part A Appl. Sci. Manuf.* **2021**, *149*, 106545.
104. Raagulan, K.; Braveenth, R.; Kim, B.M.; Lim, K.J.; Lee, S.B.; Kim, M.; Chai, K.Y. An effective utilization of MXene and its effect on electromagnetic interference shielding: Flexible, free-standing and thermally conductive composite from MXene–PAT–poly(p-aminophenol)–polyaniline co-polymer. *RSC Adv.* **2020**, *10*, 1613–1633. [CrossRef] [PubMed]
105. Liu, J.; Zhang, H.-B.; Xie, X.; Yang, R.; Liu, Z.; Liu, Y.; Yu, Z.-Z. Multifunctional, Superelastic, and Lightweight MXene/Polyimide Aerogels. *Small* **2018**, *14*, e1802479. [CrossRef] [PubMed]
106. Xu, M.K.; Liu, J.; Zhang, H.B.; Zhang, Y.; Wu, X.; Deng, Z.; Yu, Z.Z. Electrically Conductive Ti3C2Tx MXene/Polypropylene Nanocomposites with an Ultralow Percolation Threshold for Efficient Electromagnetic Interference Shielding. *Ind. Eng. Chem. Res.* **2021**, *60*, 4342–4350. [CrossRef]
107. Vu, M.C.; Mani, D.; Kim, J.B.; Jeong, T.H.; Park, S.; Murali, G.; In, I.; Won, J.C.; Losic, D.; Lim, C.S.; et al. Hybrid shell of MXene and reduced graphene oxide assembled on PMMA bead core towards tunable thermoconductive and EMI shielding nanocomposites. Compos. *Part A Appl. Sci.* **2021**, *149*, 106574. [CrossRef]
108. Wang, Y.; Liang, L.; Du, Z.; Wang, Y.; Liu, C.; Shen, C. Biodegradable PLA/CNTs/Ti3C2Tx MXene nanocomposites for efficient electromagnetic interference shielding. *J. Mater. Sci. Mater. Electron.* **2021**, *32*, 25952–25962. [CrossRef]
109. Pandey, M.; Deshmukh, K.; Pasha, S.K. Mxene-based materials for lithium–sulfur and multivalent rechargeable batteries. In *Mxenes and Their Composites*; Elsevier: Amsterdam, The Netherlands, 2022; Chapter 10; pp. 343–369.
110. Kumar, Y.R.; Deshmukh, K.; Ali, M.N.; Rajabathar, J.R.; Theerthagiri, J.; Pandey, M.; Khadheer Pasha, S.K. Structure defects and elec-tronic properties of MXenes. In *Mxenes and their Composites*; Elsevier: Amsterdam, The Netherlands, 2022; Chapter 3; pp. 91–129.

111. Shakir, M.F.; Khan, A.N.; Khan, R.; Javed, S.; Tariq, A.; Azeem, M.; Riaz, A.; Shafqat, A.; Cheema, H.M.; Akram, M.A.; et al. EMI shielding properties of polymer blends with inclusion of graphene nano platelets. *Results Phys.* **2019**, *14*, 102365. [CrossRef]
112. Hamidinejad, M.; Zhao, B.; Zandieh, A.; Moghimian, N.; Filleter, T.; Park, C.B. Enhanced Electrical and Electromagnetic Interference Shielding Properties of Polymer–Graphene Nanoplatelet Composites Fabricated via Supercritical-Fluid Treatment and Physical Foaming. *Appl. Mater. Inter.* **2018**, *10*, 30752–30761. [CrossRef]
113. Pavlou, C.; Carbone, M.G.P.; Manikas, A.C.; Trakakis, G.; Koral, C.; Papari, G.; Andreone, A.; Galiotis, C. Effective EMI shielding behaviour of thin graphene/PMMA nanolaminates in the THz range. *Nat. Commun.* **2021**, *12*, 4655. [CrossRef] [PubMed]
114. Marka, S.K.; Srikanth, V.V.S.S.; Sindam, B.; Hazra, B.K.; Raju, K.C.J.; Srinath, S. Graphene-Wrapped MgO/Poly(vinyl alcohol) Composite Sheets: Dielectric and Electromagnetic Interference Shielding Properties at Elevated Temperatures. *ACS Appl. Mater. Inter.* **2019**, *11*, 23714–23730. [CrossRef] [PubMed]
115. Ma, L.; Hamidinejad, M.; Zhao, B.; Liang, C.; Park, C.B. Layered Foam/Film Polymer Nanocomposites with Highly Efficient EMI Shielding Properties and Ultralow Reflection. *Nano-Micro Lett.* **2021**, *14*, 19. [CrossRef]
116. Sushmita, K.; Formanek, P.; Fischer, D.; Potschke, P.; Madras, G.; Bose, S. Ultrathin structures derived from interfacially modified polymeric nanocomposites to curb electromagnetic pollution. *Nanoscale Adv.* **2021**, *3*, 2632. [CrossRef] [PubMed]
117. Vineeta, S. Review of electromagnetic interference of shielding materials fabricated by iron ingredients. *Nanoscale Adv.* **2019**, *1*, 1640.
118. Liang, Z.; Julong, H.; Xingang, W.; Hongbo, W.; Zhenjun, W.; Zhuo, L.; Hongqian, Z.; Wenyu, M. Dielectric properties and electromagnetic interference shielding effectiveness of Al2O3-based composites filled with FeSiAl and flaky graphite. *J. Alloys Comp.* **2020**, *829*, 154556.
119. Khossossi, N.; Singh, D.; Ainane, A.; Ahuja, R. Recent progress of defect chemistry on 2D materials for advanced battery anodes. *Chem. Asian J.* **2020**, *15*, 3390–3404. [CrossRef]
120. Chang, M.; Jia, Z.; He, S.; Zhou, J.; Zhang, S.; Tian, M.; Wang, B.; Wu, G. Two-dimensional interface engineering of $NiS/MoS_2/Ti_3C_2T_x$ heterostructures for promoting electromagnetic wave absorption capability. *Compos. Part B Eng.* **2021**, *225*, 109306. [CrossRef]
121. Zhao, B.; Zhao, C.; Hamidinejad, M.; Wang, C.; Li, R.; Wang, S.; Yasamin, K.; Park, C.B. Incorporating a microcellular structure into PVDF/graphene–nanoplatelet composites to tune their electrical conductivity and electromagnetic interference shielding properties. *J. Mater. Chem. C* **2018**, *6*, 10292–10300. [CrossRef]
122. Fan, D.; Li, N.; Li, M.; Wang, S.; Li, S.; Tang, T. Polyurethane/polydopamine/graphene auxetic composite foam with high-efficient and tunable electromagnetic interference shielding performance. *Chem. Eng. J.* **2021**, *427*, 131635. [CrossRef]
123. Zhan, Y.; Lago, E.; Santillo, C.; Castillo, A.E.E.D.R.; Hao, S.; Buonocore, G.G.; Chen, Z.; Xia, H.; Lavorgna, M.; Bonaccorso, F. An anisotropic layer-by-layer carbon nanotube/boron nitride/rubber composite and its application in electromagnetic shielding. *Nanoscale* **2020**, *12*, 7782–7791. [CrossRef] [PubMed]
124. Liu, D.; Kong, Q.-Q.; Jia, H.; Xie, L.-J.; Chen, J.; Tao, Z.; Wang, Z.; Jiang, D.; Chen, C.-M. Dual-functional 3D multi-wall carbon nanotubes/graphene/silicone rubber elastomer: Thermal management and electromagnetic interference shielding. *Carbon* **2021**, *183*, 216–224. [CrossRef]
125. Zhang, X.; Zhang, X.; Yang, M.; Yang, S.; Wu, H.; Guo, S.; Wang, Y. Ordered multilayer film of (graphene oxide/polymer and boron nitride/polymer) nanocomposites: An ideal EMI shielding material with excellent electrical insulation and high thermal conductivity. *Compos. Sci. Technol.* **2016**, *136*, 104–110. [CrossRef]
126. Saboor, A.; Mahmood Khalid, S.; Jan, R.; Khan, A.N.; Zia, T.; Umer Farooq, M.; Afridi, S.; Sadiq, M.; Arif, M. PS/PANI/MoS2 Hybrid Polymer Composites with High Dielectric Behavior and Electrical Conductivity for EMI Shielding Ef-fectiveness. *Materials* **2019**, *12*, 2690. [CrossRef]
127. Nguyen, V.-T.; Min, B.K.; Yi, Y.; Kim, S.J.; Choi, C.-G. MXene (Ti3C2TX)/graphene/PDMS composites for multifunctional broad-band electromagnetic interference shielding skins. *Chem. Eng. J.* **2020**, *393*, 124608. [CrossRef]
128. Yadav, R.S.; Anju; Jamatia, T.; Kuřitka, I.; Vilčáková, J.; Škoda, D.; Urbánek, P.; Machovský, M.; Masař, M.; Urbánek, M.; et al. Excellent, Lightweight and Flexible Electromagnetic Interference Shielding Nanocomposites Based on Polypropylene with MnFe2O4 Spinel Ferrite Nanoparticles and Reduced Graphene Oxide. *Nanomaterials* **2020**, *10*, 2481. [CrossRef]
129. Zubair, K.; Ashraf, A.; Gulzar, H.; Shakir, H.M.F.; Nawab, Y.; Rehan, Z.A.; Rashid, I.A. Study of mechanical, electrical and EMI shielding properties of polymer-based nanocomposites incorporating polyaniline coated graphene nanoparticles. *Nano Express* **2021**, *2*, 010038. [CrossRef]
130. Gao, Z.; Zhang, J.; Zhang, S.; Lan, D.; Zhao, Z.; Kou, K. Strategies for electromagnetic wave absorbers derived from zeolite imidazole framework (ZIF-67) with ferrocene containing polymers. *Polymer* **2020**, *202*, 122679. [CrossRef]
131. Liang, C.; Qiu, H.; Han, Y.; Gu, H.; Song, P.; Wang, L.; Kong, J.; Cao, D.; Gu, J. Superior electromagnetic interference shielding 3D graphene nanoplatelets/reduced graphene oxide foam/epoxy nanocomposites with high thermal conductivity. *J. Mater. Chem. C* **2019**, *7*, 2725–2733. [CrossRef]
132. Yousefi, N.; Sun, X.; Lin, X.; Shen, X.; Jia, J.; Zhang, B.; Tang, B.; Chan, M.; Kim, J.-K. Highly Aligned Graphene/Polymer Nanocomposites with Excellent Dielectric Properties for High-Performance Electromagnetic Interference Shielding. *Adv. Mater.* **2014**, *26*, 5480–5487. [CrossRef]
133. Shen, B.; Zhai, W.; Tao, M.; Ling, J.; Zheng, W. Lightweight, Multifunctional Polyetherimide/Graphene@Fe3O4 Composite Foams for Shielding of Electromagnetic Pollution. *ACS Appl. Mater. Inter.* **2013**, *5*, 11383–11391. [CrossRef] [PubMed]

134. Zhang, H.B.; Yan, Q.; Zheng, W.G.; He, Z.; Yu, Z.Z. Tough Graphene-Polymer Microcellular Foams for Electromagnetic Interference Shielding. *ACS Appl. Mater. Inter.* **2011**, *3*, 918–924. [CrossRef]
135. Yao, B.; Hong, W.; Chen, T.; Han, Z.; Xu, X.; Hu, R.; Hao, J.; Li, H.; Perini, S.E.; Lanagan, M.T.; et al. Highly Stretchable Polymer Composite with Strain-Enhanced Electromagnetic Interference Shielding Effectiveness. *Adv. Mater.* **2020**, *5*, 1907499. [CrossRef]
136. Wu, X.; Han, B.; Zhang, H.B.; Xie, X.; Tu, T.; Zhang, Y.; Dai, Y.; Yang, R.; Yu, Z.Z. Compressible, durable and conductive polydi-methylsiloxane-coated MXene foams for high-performance electromagnetic interference shielding. *Chem. Eng. J.* **2020**, *381*, 122622. [CrossRef]
137. Cheng, Y.; Li, X.; Qin, Y.; Fang, Y.; Liu, G.; Wang, Z.; Matz, J.; Dong, P.; Shen, J.; Ye, M. Hierarchically porous polyimide/$Ti_3C_2T_x$ film with stable electromagnetic interference shielding after resisting harsh conditions. *Sci. Adv.* **2021**, *7*, eabj1663. [CrossRef] [PubMed]
138. Sun, R.; Zhang, H.B.; Liu, J.; Xie, X.; Yang, R.; Li, Y.; Hong, S.; Yu, Z.Z. Highly Conductive Transition Metal Carbide/Carbonitride(MXene)@polystyrene Nanocomposites Fabricated by Assembly for Highly Efficient Electromagnetic Inter-ference Shielding. *Adv. Funct. Mater.* **2017**, *27*, 1702807. [CrossRef]
139. Shi, Y.-D.; Li, J.; Tan, Y.-J.; Chen, Y.-F.; Wang, M. Percolation Behavior of Electromagnetic Interference Shielding in Poly-mer/Multi-Walled Carbon Nanotube Nanocomposites. *Compos. Sci. Technol.* **2019**, *170*, 70–76. [CrossRef]
140. Ashraf, M.A.; Peng, W.; Zare, Y.; Rhee, K.Y. Effects of Size and Aggregation/Agglomeration of Nanoparticles on the Interfacial/Interphase Properties and Tensile Strength of Polymer Nanocomposites. *Nanoscale. Res. Lett.* **2018**, *13*, 214. [CrossRef] [PubMed]
141. Yang, X.; Fan, S.; Li, Y.; Qiang, Y.; Li, Y.; Ruan, K.; Zhang, S.; Zhang, J.; Kong, J.; Gu, J. Synchronously improved electromagnetic interference shielding and thermal conductivity for epoxy nanocompo-sites by constructing 3D copper nanowires/thermally annealed graphene aerogel framework. *Compos. Appl. Sci. Manuf.* **2020**, *128*, 105670. [CrossRef]